



ELSEVIER

Contents lists available at SciVerse ScienceDirect

Journal of Theoretical Biology

journal homepage: www.elsevier.com/locate/jtbi

Signatures of nonlinearity in single cell noise-induced oscillations

Philipp Thomas^{a,b,c}, Arthur V. Straube^c, Jens Timmer^d, Christian Fleck^{f,g}, Ramon Grima^{a,e,*}^a School of Biological Sciences, University of Edinburgh, United Kingdom^b School of Mathematics, University of Edinburgh, United Kingdom^c Department of Physics, Humboldt University of Berlin, Germany^d BIOS Centre for Biological Signalling Studies, University of Freiburg, Germany^e Freiburg Institute for Advanced Studies, University of Freiburg, Germany^f Laboratory for Systems and Synthetic Biology, Wageningen University, Netherlands^g Centre for Biological Systems Analysis (ZBSA), University of Freiburg, Germany

HIGHLIGHTS

- We develop a general theory of noise-induced oscillations in subcellular volumes.
- The theory provides the power spectrum in closed form for any monostable network.
- The spectra close to a Hopf bifurcation have three universal features.
- The predicted features are seen in experimental single cell data.
- Simulations of circadian and mitotic oscillators verify the theory's accuracy.

ARTICLE INFO

Article history:

Received 10 January 2013

Received in revised form

20 May 2013

Accepted 18 June 2013

Available online 2 July 2013

Keywords:

Master equations

Stochastic differential equations

Oscillations

Linear noise approximation

Intrinsic noise

ABSTRACT

A class of theoretical models seeks to explain rhythmic single cell data by postulating that they are generated by intrinsic noise in biochemical systems whose deterministic models exhibit only damped oscillations. The main features of such noise-induced oscillations are quantified by the power spectrum which measures the dependence of the oscillatory signal's power with frequency. In this paper we derive an approximate closed-form expression for the power spectrum of any monostable biochemical system close to a Hopf bifurcation, where noise-induced oscillations are most pronounced. Unlike the commonly used linear noise approximation which is valid in the macroscopic limit of large volumes, our theory is valid over a wide range of volumes and hence affords a more suitable description of single cell noise-induced oscillations. Our theory predicts that the spectra have three universal features: (i) a dominant peak at some frequency, (ii) a smaller peak at twice the frequency of the dominant peak and (iii) a peak at zero frequency. Of these, the linear noise approximation predicts only the first feature while the remaining two stem from the combination of intrinsic noise and nonlinearity in the law of mass action. The theoretical expressions are shown to accurately match the power spectra determined from stochastic simulations of mitotic and circadian oscillators. Furthermore it is shown how recently acquired single cell rhythmic fibroblast data displays all the features predicted by our theory and that the experimental spectrum is well described by our theory but not by the conventional linear noise approximation.

© 2013 Elsevier Ltd. All rights reserved.

1. Introduction

Cellular rhythms are ubiquitous throughout many tissues of the body (Mohawk et al., 2012). The central pacemaker of the mammalian circadian clock located in the suprachiasmatic nucleus is thought to be entrained to a light-dark cycle and to reset the

* Corresponding author at: C. H. Waddington Building, Mayfield Road, University of Edinburgh, EH9 3JD, UK. Tel.: +44 131 651 9060.

E-mail address: Ramon.Grima@ed.ac.uk (R. Grima).

expression of clock genes in peripheral tissues in vivo (Mohawk et al., 2012). For example, 10% of the transcriptome and 20% of the proteome in mouse liver are expressed rhythmically (Panda et al., 2002; Reddy et al., 2006). Similar fractions have been found to be under circadian control in the human metabolome indicating that rhythmic expression of clock genes controls many downstream pathways (Dallmann et al., 2012).

In the absence of pacemaker control, isolated peripheral clocks function as sustained but independently phased cell autonomous 24 h-oscillators under constant light conditions (Welsh et al., 2004; Nagoshi et al., 2004). In consequence initially synchronized

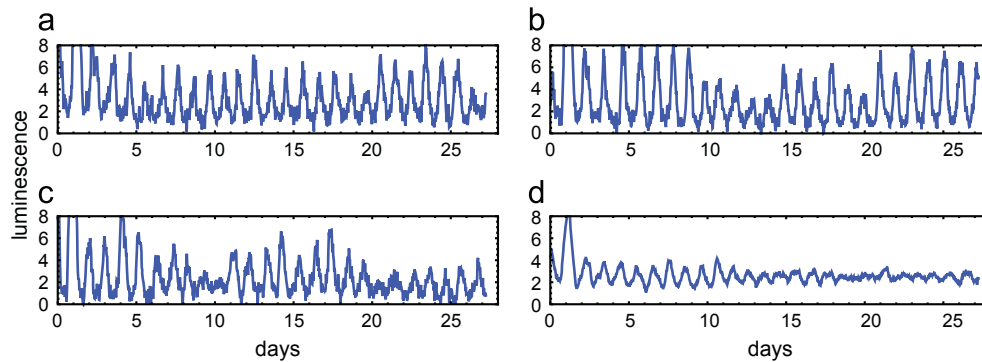


Fig. 1. Single cell circadian oscillations in individual fibroblast cells over two weeks after medium change reproduced from experimental dataset S1 in Leise et al. (2012). (a–c) Single time course of protein luminescence of first three individual fibroblast cells shows sustained oscillations. (d) Population average over the first 20 cells shows a dampening of the oscillations due to dephasing of individual cell rhythms.

cell cultures display only damped oscillations on the ensemble level due to a gradual dephasing of individual cellular clocks (Welsh et al., 2004; Westermark et al., 2009). Fig. 1 illustrates this phenomenon by comparing three time traces of protein luminescence (a–c) from single fibroblast cells against the averaged response of a culture of 20 cells shown in (d). The images have been reproduced from dataset S1 in Leise et al. (2012).

It is still under debate what is the underlying single cell mechanism responsible for producing oscillations. In the absence of noise, populations of synchronized self-sustained oscillators exhibit in-phase oscillations of constant amplitude while populations of damped oscillators show an in-phase decaying amplitude. In both cases, taking into account the molecular fluctuations stemming from the stochastic nature of the underlying biochemical reactions leads to a population of cells with sustained (noisy) oscillations and with cell-to-cell variation in the phase. Hence presently experimental single cell data can be explained by both noisy self-sustained and damped oscillator models (Westermark et al., 2009).

The fact that molecular noise induces a deterministically damped oscillator to exhibit sustained oscillations has led to this phenomenon being called noise-induced oscillations (NIOs) (Vilar et al., 2002; McKane et al., 2007). The amplitude of these oscillations is proportional to $1/\sqrt{N}$ where N is the mean number of molecules. Hence NIOs have been deemed important for reactions involving a typically small number of molecules such as those occurring inside cells (Grima and Schnell, 2008). Similar mechanisms to generate NIOs have been described as coherence resonance with non-excitable dynamics in the contexts of epidemics (Kuske et al., 2007), predator–prey interactions (Rozenfeld et al., 2001) and lasers models (Ushakov et al., 2005).

The power spectrum of concentration fluctuations has been the main measure used to quantify NIOs, both experimentally and theoretically, to date (Gang et al., 1993; Hou and Xin, 2003; Welsh et al., 2004; Davis and Roussel, 2006; Li and Lang, 2008; Geva-Zatorsky et al., 2010; Ko et al., 2010). Briefly speaking the power spectrum measures how the square amplitude of a signal is distributed with frequency. In particular, peaks in the power spectrum indicate the presence of NIOs. For systems composed of purely first-order reactions, exact expressions for the power spectrum of concentration fluctuations can be derived from the chemical master equation (CME) (the accepted mesoscopic description of biochemical kinetics) (Warren et al., 2006; Simpson et al., 2004). However, most biochemical systems of interest do not fall in the latter category since they are composed of a large number of bimolecular reactions arising from oligomer binding, cooperativity, allostery or phosphorylation of proteins (Novák and Tyson, 2008). A popular means to obtain approximate expressions for the power spectra of systems composed of both

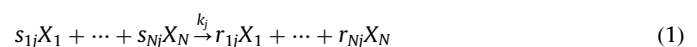
unimolecular and bimolecular reactions is the linear noise approximation (LNA) of the CME (Van Kampen, 1976; Dauxois et al., 2009; McKane et al., 2007; Qian, 2011; Toner and Grima, 2013) whereby the probability distribution solution of the CME is approximated by a Gaussian. It is, however, the case that the LNA provides a good approximation to the CME only in the limit of large volumes at constant concentrations, i.e., the limit of large molecule numbers. Given that molecule numbers of several key intracellular players are in the range of few tens to several thousands (Schwanhäusser et al., 2011), it is plausible that the predictions of the LNA maybe limited in scope for biological systems. Indeed recent studies (Grima, 2009, 2010, 2012; Thomas et al., 2010; Ramaswamy et al., 2012) have shown that the mean concentrations and variances of interacting chemical species present in low molecule number can be considerably different than those given by the LNA; these effects originate from the combination of intrinsic noise and nonlinearity in the law of mass action. Similarly analytical studies of two-variable epidemic (Chaffee and Kuske, 2011) and predator–prey models (Scott, 2012) revealed NIOs with more than one frequency that are not captured by linear analysis. While it is clear that the LNA must miss some of the crucial features of single cell NIOs, a thorough investigation of these effects has not been carried out to-date.

In this paper we obtain the leading order correction to the LNA's prediction of the power spectrum of the fluctuations for a general biochemical reaction pathway whose corresponding deterministic system is just below a super-critical Hopf bifurcation. We show that this novel nonlinear contribution to the power spectrum yields additional peaks at zero frequency and at twice the frequency of the peak predicted by the LNA. The analytical results are verified by comparison with experimental single cell data of rhythmic fibroblast cells and with detailed stochastic simulations of an oscillator controlling mitosis and of a transcriptional feedback oscillator.

2. Preliminaries: linear theory of noise-induced oscillations

2.1. The standard description of stochastic chemical kinetics

We consider a general chemical system consisting of a number N of distinct chemical species interacting via R chemical reactions of the type



occurring in a volume of mesoscopic size Ω . Here j is an index running from 1 to R , X_i denotes chemical species i , s_{ij} and r_{ij} are the stoichiometric coefficients and k_j is the rate constant of the j th reaction. Under well-mixed conditions there are two descriptions

that have been commonly employed to describe such systems. In the first approach the time-dependent concentrations $\phi = (\phi_1, \dots, \phi_N)^T$ are obtained from the solution of deterministic rate equations (REs):

$$\frac{\partial}{\partial t} \phi = \mathbf{f}(\phi). \quad (2)$$

In the second approach the mesoscopic state is given by a vector of population numbers $\mathbf{n} = (n_1, \dots, n_N)^T$ drawn from a probability distribution. The time evolution equation of this probability $\Pi(\mathbf{n}, t)$ is given by the CME (Gillespie, 2007; van Kampen, 2007):

$$\frac{\partial \Pi(\mathbf{n}, t)}{\partial t} = \sum_{j=1}^R (a_j(\mathbf{n}-\mu_j)\Pi(\mathbf{n}-\mu_j, t) - a_j(\mathbf{n})\Pi(\mathbf{n}, t)). \quad (3)$$

where $a_j(\mathbf{n})dt$ is the probability that the j th reaction occurs within infinitesimal time dt and the state \mathbf{n} changes to $\mathbf{n} + \mu_j$ where $\mu_j = (r_{1j} - s_{1j}, r_{2j} - s_{2j}, \dots, r_{Nj} - s_{Nj})$. Following Gillespie (2007) we shall refer to μ_j as the state-change vector for the j th reaction. It has been shown that the relation between the functions \mathbf{f} and the propensities a_j is given by the macroscopic limit $\mathbf{f}(\phi) = \lim_{\Omega \rightarrow \infty} \sum_j \mu_j a_j(\Omega\phi)/\Omega$ in which both descriptions, Eqs. (2) and (3), are equivalent (van Kampen, 2007; Thomas et al., 2012). It is, however, well appreciated that this limit does not accurately capture the dynamics of biochemical reactions in individual cells but rather resembles more closely the average over populations of identical cells.

The discrepancy between the two approaches stems from the fact that the deterministic approach assumes the molecule numbers in a cell to be sufficiently large while the stochastic one suffers no such restriction. A popular method to simulate stochastic time traces distributed according to the solution of Eq. (3) is the stochastic simulation algorithm (SSA) as introduced by Gillespie. Such simulations are widely used to show off qualitative deviations from the deterministic description such as the existence of noise-induced oscillations which were indeed observed in Gillespie's seminal paper introducing the SSA (Gillespie, 1977).

As mentioned in the Introduction, NIOs are quantified by means of the power spectrum of concentration fluctuations. This is formally defined as follows. The autocorrelation function of the s th species is given by

$$\Sigma_s(\tau) = \left\langle \left(\frac{n_s(t) - \langle n_s \rangle}{\Omega} \right) \left(\frac{n_s(t + \tau) - \langle n_s \rangle}{\Omega} \right) \right\rangle, \quad (4)$$

which allows to identify periodicities present in individual realizations $n_s(t)$ of the stochastic process. Note that the angled brackets denote the ensemble average and t is any time for which the system has achieved steady-state. The power spectral density of fluctuations is then defined by the Fourier transform of the autocorrelation function

$$P_s(\omega) = \int_{-\infty}^{\infty} d\tau e^{-i\omega\tau} \Sigma_s(\tau), \quad (5)$$

such that $P_s(\omega)d\omega/(2\pi)$ is the power contained in the infinitesimal frequency interval $d\omega/(2\pi)$. For brevity we refer to Eq. (5) simply as the power spectrum of the concentration fluctuations of species s .

2.2. Power spectra within the linear noise approximation

While the power spectrum Eq. (5) is easy to obtain experimentally or to calculate from stochastic simulations using the SSA, it is not generally possible to obtain exact expressions for it unless the system is composed of only unimolecular reactions (Warren et al., 2006). The use of the LNA bypasses this difficulty, and we next briefly review this approach (for more details see the section Methods).

The LNA has been derived by van Kampen using the system size expansion (van Kampen, 2007) and has been subsequently extensively used to quantify NIOs by others. The LNA result states that in the limit of large molecule numbers, the fluctuating concentration predicted by the CME for a single cell is approximately equal to a sum of two terms: a contribution describing the population average $\phi(t)$ given by the REs, Eq. (2), and another contribution describing fluctuations $\epsilon(t)$ about them in a single cell:

$$\frac{\mathbf{n}(t)}{\Omega} = \phi(t) + \epsilon(t), \quad (6)$$

where the time-evolution of the fluctuations $\epsilon(t)$ is given by the linear Langevin equation

$$\frac{d}{dt} \epsilon(t) = \underline{J}(\phi(t))\epsilon(t) + \Omega^{-1/2} \underline{B}(\phi(t))\Gamma(t), \quad (7)$$

where the matrix \underline{J} denotes the Jacobian of the deterministic equation, Eq. (2), the elements of the matrix \underline{B} read $B_{ij} = \Omega^{-1/2} \mu_{ij} \sqrt{a_j(\Omega\phi)}$ where μ_{ij} is the i th component of the vector μ_j and the R -dimensional vector Γ is Gaussian white noise satisfying $\langle \Gamma_i(t)\Gamma_j(t') \rangle = \delta_{ij}\delta(t-t')$ for each pair of reactions. Note that underlined symbols represent matrices throughout the paper. Note also that our notation is slightly different than the one used by van Kampen where the quantity $\epsilon(t)$ has been rescaled by a factor of $\Omega^{1/2}$ (see van Kampen, 2007, Chapter X).

It can be shown by taking the Fourier transform of Eq. (7) that the power spectrum of fluctuations in species s is given by

$$P_s^{\text{LNA}}(\omega) = \frac{1}{\Omega} [(\underline{J} - i\omega)^{-1} \underline{B} \underline{B}^T (\underline{J} + i\omega)^{-1}]_{ss}, \quad (8)$$

which can be more usefully written using the eigenrepresentation of the Jacobian

$$P_s^{\text{LNA}}(\omega) = \frac{1}{\Omega} \sum_{ij} U_{si}^{-1} \frac{[\underline{B} \underline{B}^T]_{ij}}{(\lambda_i - i\omega)(\lambda_j^* + i\omega)} U_{js}^{-\dagger}, \quad (9)$$

where \underline{U}^{-1} is the matrix of eigenvectors of \underline{J} and the λ 's are its eigenvalues, as given by the relationship $\underline{U} \underline{J} \underline{U}^{-1} = \text{diag}(\lambda_1, \lambda_2, \dots, \lambda_N)$. The matrix \underline{B} is defined as equal to $\underline{U} \underline{B}$. Note that \underline{U}^{-1} is shorthand notation for $(\underline{U}^{-1})^\dagger$. By inspection of the above equation one can deduce that when there exists a pair of complex conjugate eigenvalues the dependence of the denominator can yield a Lorentzian peak at a nonzero frequency which is the signature of a NIO (McKane et al., 2007).

In what follows we assume that the eigenvalue spectrum of the Jacobian \underline{J} is composed of a pair of conjugate eigenvalues $\lambda_1 = -\gamma + i\omega_0$, $\lambda_2 = -\gamma - i\omega_0$ and $N-2$ real negative eigenvalues λ_i where $i = 3, \dots, N$. The deterministic dynamics then corresponds to a focus which becomes unstable as $\gamma \rightarrow 0$, i.e., the Hopf bifurcation point. In particular, by considering the dominant term in Eq. (9) (corresponding to $i=j=1$), one can deduce that the power spectrum has a peak at $\omega \approx \omega_0$ whenever

$$\frac{\gamma}{\omega_0} \ll 1, \quad (10)$$

i.e., the phenomenon of NIO becomes particularly conspicuous when the deterministic dynamics is close to a critical point giving rise to a limit cycle through a Hopf bifurcation (Ushakov et al., 2005). In this case the total power is concentrated in the peak and can be approximated by the peak height ($\sim G/(\Omega\gamma^2)$), where $G = [\underline{B} \underline{B}^T]_{11}$, multiplied by its spectral width ($\sim \gamma$), is of the order

$$\frac{G}{\Omega\gamma}. \quad (11)$$

Since the total power is equal to the variance of the NIO it follows that Eq. (11) needs to be sufficiently small for the LNA to hold. Similar criteria have been obtained using multiple scale analysis in Kuske et al. (2007) (see Eq. (24) therein). In the same limit the

sample paths of Eq. (7) can be interpreted as given by a fast oscillation with frequency ω_0 whose amplitude is stochastically modulated on the slow timescale $1/\gamma$ (Baxendale and Greenwood, 2011).

3. Results: nonlinear theory of noise-induced oscillations

Biochemical networks are typically composed of nonlinear (bimolecular) reactions whose stochastic kinetics is not accounted for insufficiently by linear analysis; in particular the first and second moments of intrinsic noise as given by the LNA become inaccurate for nonlinear systems with small molecule numbers (Grima, 2010, 2012; Thomas et al., 2012). In this section we sketch the derivation of an approximate equation for the power spectrum of concentration fluctuations close to the bifurcation point using a nonlinear stochastic differential equation (SDE) which predicts behavior qualitatively different from that obtained by linear theory. In Fig. 2 we illustrate the main steps to arrive at the central result Eq. (20) by graphic means, in particular we emphasize how distinct features of the power spectrum arise from different orders of approximation. For a complete derivation we refer the reader to the section Methods.

Our starting point is the chemical Langevin equation (CLE)

$$\frac{d}{dt}\mathbf{x}(t) = \mathbf{f}(\mathbf{x}(t)) + \Omega^{-1/2}\mathbf{B}(\mathbf{x}(t))\mathbf{\Gamma}(t), \tag{12}$$

which is the nonlinear (Ito) SDE derived from a normal approximation of the Poisson increments of the underlying discrete process sampled by the SSA (Kurtz, 1976; Gillespie, 2000; Allen et al., 2008). Note that here $\mathbf{x} = \mathbf{n}/\Omega$ is the vector of mesoscopic concentrations, $\mathbf{f}(\mathbf{x}) = \Omega^{-1}\sum_{j=1}^R \mu_j a_j(\Omega\mathbf{x})$ is the drift vector, \mathbf{B} is the noise matrix with elements $B_{ij}(\mathbf{x}) = \Omega^{-1/2} \mu_{ij} \sqrt{a_j(\Omega\mathbf{x})}$ and the vector $\mathbf{\Gamma}$ is Gaussian white noise as before. The use of the nonlinear SDE as a means to go beyond the linear SDE of the LNA is further motivated by a recent study showing that the relative error between the first two moments of the nonlinear SDE and of the SSA is merely of the order of a few percent for monostable systems with few tens of molecules (Grima et al., 2011). In the section Applications we have verified the validity of this approximation by comparing its estimates for the power spectrum against that obtained from the SSA for two biologically relevant examples.

In the limit of large molecule numbers (the limit of large volumes at constant concentration), the CLE reduces to the conventional deterministic REs given by Eq. (2) and the LNA, Eq. (7), accounting for the fluctuations (Grima et al., 2011; Wallace et al., 2012). As previously mentioned, for intermediate molecule numbers, Eq. (12) has been shown to be more accurate than the LNA, however, the nonlinear character of the equation which is responsible for its higher accuracy, also prevents one from finding an exact solution. Nonlinearity enters the CLE through two coefficients accounting for drift and noise amplitude. We now seek a small noise expansion which is different from the usual LNA by the fact that it retains enough terms to ensure both coefficients remain non-singular as the bifurcation point is approached.

Assuming steady state conditions we can make a small noise ansatz $\mathbf{x}(t) = \boldsymbol{\phi} + \epsilon(t)$ which separates the dynamics into deterministic and stochastic parts and which is valid since the deterministic system is monostable (van Kampen, 2007). In order to investigate the dependence of the drift term in Eq. (12) close to the bifurcation point we make use of the transformation matrix \mathbf{U} to obtain the expansion in the eigenrepresentation of the Jacobian. Including terms up to quadratic order in $\tilde{\epsilon} = \mathbf{U}\epsilon$ the result is given by

$$\sum_{\alpha} U_{i\alpha} f_{\alpha}(\mathbf{x}) = \sum_{\alpha} U_{i\alpha} f_{\alpha}(\boldsymbol{\phi}) + \lambda_i \tilde{\epsilon}_i + \frac{1}{2} \sum_{\alpha\beta} \tilde{J}_i^{\alpha\beta}(\boldsymbol{\phi}) \tilde{\epsilon}_{\alpha} \tilde{\epsilon}_{\beta} + \dots \tag{13}$$

where the new symbol introduced in the third term is given by

$$\tilde{J}_i^{\alpha\beta}(\boldsymbol{\phi}) = \sum_{\mu\nu} U_{\mu i}^{-1} U_{\nu i}^{-1} U_{i\alpha} \frac{\partial^2 f_{\alpha}(\boldsymbol{\phi})}{\partial \phi_{\mu} \partial \phi_{\nu}}. \tag{14}$$

Note that the tilde stands for quantities in the eigenrepresentation of the Jacobian. Note also that the above expression is a function of the Hessian of the rate equations, $J_{\alpha}^{\mu\nu} = \partial^2 f_{\alpha}(\boldsymbol{\phi}) / (\partial \phi_{\mu} \partial \phi_{\nu})$, and hence is non-zero whenever $f_{\alpha}(\boldsymbol{\phi})$ is nonlinear; this is the case when the α th species is involved in bimolecular or higher-order reactions. Considering Eq. (13) we note that the first term is zero because we are in steady state conditions, i.e., $\mathbf{f}(\boldsymbol{\phi}) = 0$. In the vicinity of the Hopf bifurcation, for $i=1,2$, the real parts of the eigenvalues of the Jacobian given by $-\gamma$ entering the second term become very small

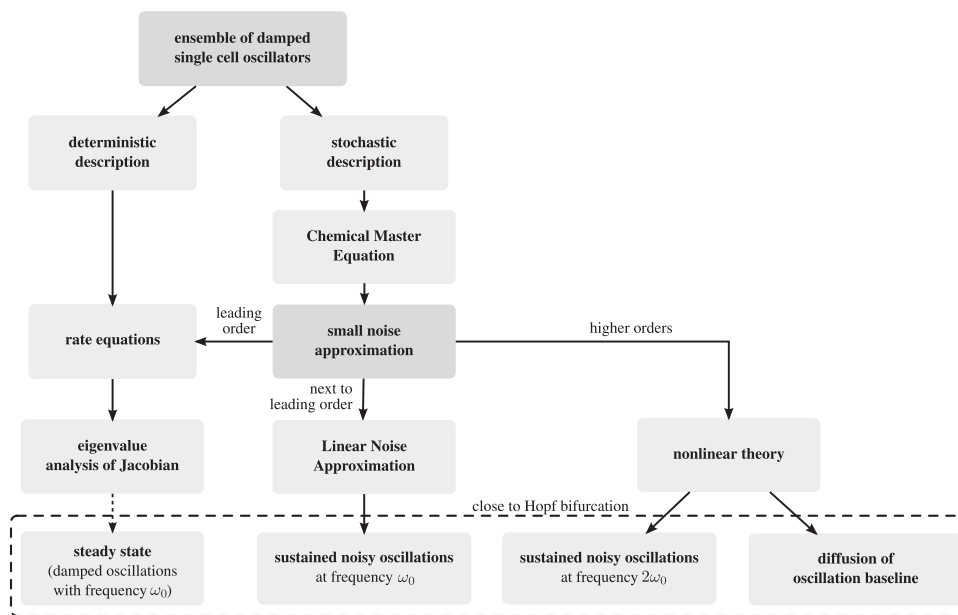


Fig. 2. Schematic illustrating how different levels of approximation lead to distinct features in the power spectrum of single cell noise-induced oscillations. In particular, the LNA describes sustained NIOs at a frequency ω_0 which is the same as the frequency of the damped oscillations in the deterministic description. The nonlinear SDE approach leads to an additional second harmonic of the fundamental frequency and a diffusion of the baseline of oscillations close to the Hopf bifurcation.

and hence the real parts of the third term dominate. Thus up to second-order terms must be retained to guarantee that the drift coefficient is not singular as the bifurcation point is approached. In contrast, for the noise coefficient the leading order contribution is sufficient since the first term in its expansion, $\tilde{B}_{ia}(\phi)$ is non-zero at the bifurcation. Hence using the eigenrepresentation of the Jacobian the nonlinear Langevin equation, Eq. (12), can be approximated as

$$\partial_t \tilde{\epsilon}_i(t) = \lambda_i \tilde{\epsilon}_i + \frac{1}{2} \sum_{\alpha\beta} \tilde{J}_i^{\alpha\beta}(\phi) \tilde{\epsilon}_\alpha \tilde{\epsilon}_\beta + \Omega^{-1/2} \sum_\alpha \tilde{B}_{ia}(\phi) \Gamma_\alpha(t), \quad (15)$$

close to the bifurcation point. Still, the power spectrum of the above Langevin equation cannot be obtained straightforwardly since the nonlinear character of the equation is retained and hence to proceed further an approximation method becomes indispensable. We now substitute the Fourier transform

$$\tilde{\epsilon}_i(t) = \int_{-\infty}^{\infty} \frac{d\omega}{2\pi} e^{i\omega t} \hat{\epsilon}_i(\omega), \quad (16)$$

into Eq. (15) and expand $\hat{\epsilon}_i$ in powers of the inverse square root of the system size

$$\hat{\epsilon}_i(\omega) = \Omega^{-1/2} \hat{\epsilon}_i^{(0)}(\omega) + \Omega^{-1} \hat{\epsilon}_i^{(1)}(\omega) + O(\Omega^{-3/2}). \quad (17)$$

After equating terms of order $\Omega^{-1/2}$ and subsequently those of order Ω^{-1} one finds that the power spectrum of the s th species expressed in the eigenrepresentation of the Jacobian is given by

$$P_s(\omega) = P_s^{\text{LNA}}(\omega) + \frac{1}{\Omega^2} \underline{U}^{-1} \langle (\hat{\epsilon}^{(1)}(\omega) \hat{\epsilon}^{(1)\dagger}(\omega)) - \delta(\omega) \langle \hat{\epsilon}^{(1)} \rangle \langle \hat{\epsilon}^{(1)T} \rangle \rangle \underline{U}^{-\dagger}, \quad (18)$$

where the first term is related to the spectrum of $\hat{\epsilon}_i^{(0)}(\omega)$ by $P_s^{\text{LNA}}(\omega) = \underline{U}^{-1} \langle \hat{\epsilon}^{(0)}(\omega) \hat{\epsilon}^{(0)\dagger}(\omega) \rangle \underline{U}^{-\dagger}$ and is exactly equivalent to Eq. (9) obtained by the LNA while the second is a correction term related to the spectrum of $\hat{\epsilon}_i^{(1)}(\omega)$ accounting for nonlinear effects in Langevin equation (15).

As shown in the Methods section, Eq. (18) simplifies to

$$P_s(\omega) = \frac{1}{\Omega} \sum_{ij} U_{si}^{-1} \frac{[\tilde{B}\tilde{B}^\dagger]_{ij}}{(\lambda_i - i\omega)(\lambda_j^* + i\omega)} U_{js}^{-\dagger} - \frac{1}{2\Omega^2} \sum_{ij} \sum_{\alpha\beta\mu\nu} U_{si}^{-1} \tilde{J}_i^{\alpha\beta} \tilde{\sigma}_{\alpha\mu} \left(\frac{1}{\lambda_\alpha + \lambda_\beta - i\omega} + \frac{1}{\lambda_\mu^* + \lambda_\nu^* + i\omega} \right) \times \frac{\tilde{J}_j^{*\mu\nu} \tilde{\sigma}_{\nu\beta}^*}{(\lambda_j^* + i\omega)} U_{js}^{-\dagger} + O(\Omega^{-5/2}), \quad (19)$$

where $\tilde{\sigma}_{ij} = -[\tilde{B}\tilde{B}^\dagger]_{ij}/(\lambda_i + \lambda_j^*)$ is the LNA covariance matrix of the eigenmodes. The above expression is the spectrum of the nonlinear Langevin equation (15) accurate to order Ω^{-2} . The latter as we have argued approximates the CME in the limit of large population numbers close to the Hopf bifurcation point. In the Methods section we have shown that close to the bifurcation, the covariance of the near-critical eigenmodes is diagonally dominant, i.e., $\tilde{\sigma}_{ij} \approx \delta_{ij} G/(2\gamma)$ (for i and j equal to 1 or 2) with $G = [\tilde{B}\tilde{B}^\dagger]_{11} = [\tilde{B}\tilde{B}^\dagger]_{22}$ and hence these yield the major contributions to the sum. Given this reasoning we can write the power spectrum of the concentration fluctuations of species s close to the bifurcation:

$$P_s(\omega) \approx P_s^{\text{LNA}}(\omega) + \frac{\Omega^{-2} G^2}{2\gamma} \left(\frac{|M_s^{11}(\omega)|^2}{(\omega - 2\omega_0)^2 + (2\gamma)^2} + 2 \frac{|M_s^{12}(\omega)|^2}{\omega^2 + (2\gamma)^2} \right), \quad (20)$$

where non-resonant contributions have been omitted. The coefficients in the above expression are given by

$$M_s^{ij}(\omega) = \sum_{\alpha\mu} [(\underline{J} - i\omega)^{-1}]_{sa} U_{\mu i}^{-1} U_{\alpha j}^{-1} \frac{\partial^2 f_\alpha(\phi)}{\partial \phi_\mu \partial \phi_\nu}. \quad (21)$$

The first term in Eq. (20) is the prediction of the LNA which leads to a peak at $\omega = \omega_0$. Specifically, the second term in Eq. (20) leads to a peak at twice the LNA frequency $\omega = 2\omega_0$, and the third term leads to a peak at zero frequency $\omega = 0$ whenever we are close to the Hopf bifurcation point. These extra peaks are due to the combined influence of noise and nonlinearity of the chemical reactions. As argued in the previous section the fundamental peak gives a contribution of order $G/(\Omega\gamma)$ to the overall variance; similarly it can be shown that the total power concentrated in the additional two peaks is of order

$$\left(\frac{G}{\Omega\gamma} \right)^2. \quad (22)$$

It hence follows that the corrections in Eq. (20) become significant when $G/\Omega \approx \gamma$, i.e., when there exists a balance between the noise coefficient G/Ω and the distance from the bifurcation point γ . The conditions for the observability of the additional peaks at twice the frequency of the principal peak and at zero frequency require

$$|M_s^{11}(2\omega_0)| \neq 0, \quad |M_s^{12}(0)| \neq 0, \quad (23)$$

respectively. Using the above together with Eq. (21) it follows that the Hessian of the corresponding deterministic system $\partial^2 f_\alpha(\phi)/(\partial \phi_\mu \partial \phi_\nu)$ needs to be non-zero at the bifurcation point; however, this condition is not sufficient. Assuming that $|M_s^{11}(2\omega_0)|$ is a continuous function of ω_0 then clearly the first condition in Eq. (23) is fulfilled for all values of $2\omega_0$ except the zeros of M_s^{11} which depend on the specific rate constants of the network under consideration. The second condition in Eq. (23) is independent of ω_0 and is as we show in the next section not generally true for all biochemical processes of interest.

The physical meaning of the peak at zero frequency is not as intuitive as the peaks at non-zero frequency and requires further explanation. Given that γ is very small (since we are close to the Hopf bifurcation) and assuming that $M_s^{12}(0) \neq 0$ then it follows that the spectrum associated with the last term on the right hand side of Eq. (20) is approximately proportional to $|M_s^{12}(0)|^2 \omega^{-2}$ for $\omega_0 \gg \omega \gg \gamma$. A spectrum characterized by this scaling form is associated with random walk noise; to be more precise, given a Langevin equation $\partial_t x(t) = \sqrt{2D}\Gamma(t)$ where D is the diffusion coefficient and $\Gamma(t)$ is white noise, then the power spectrum of the signal $x(t)$ is equal to $2D/\omega^2$. Thus it follows that the fluctuating signal whose spectrum is given by Eq. (20) can be interpreted as the sum of the three components: (i) a component which fluctuates about the mean with diffusion coefficient $|M_s^{12}(0)|^2 G^2/(2\Omega^2\gamma)$; (ii) a noisy component with power concentrated at a frequency of ω_0 ; (iii) another oscillatory component as (ii) but with power concentrated at a frequency of $2\omega_0$. These components are, respectively, associated with the spectra given by the last term, the first term and the second term on the right hand side of Eq. (20). We also note that the integral of Eq. (20) over ω gives the variance of the fluctuations in species s close to the bifurcation; this is a sum of the variance predicted by the LNA and a correction term of order Ω^{-2} . The latter is always positive and hence it can be stated that to the order of the approximation used, the LNA invariably underestimates the variance close to a Hopf bifurcation.

In the next section we apply our theory to the three cases of biological interest. In particular we show how the theory can be used to explain recently obtained experimental single cell rhythm data and also illustrate by means of two examples how one calculates Eq. (20) for a given system of interest. Stochastic simulations using the SSA are used to verify the accuracy of our theory for intermediate volumes and also to probe small volume phenomena which are beyond its predictive power.

4. Applications

4.1. Noise-induced oscillations observed in individual fibroblast cells

Recently, *Leise et al. (2012)* reported experimental protein luminescence data from cultures of 80 highly rhythmic fibroblast cells. Single cell spectra were obtained from individual observations over a six week period and averaged over the cell population. This data (see dataset S1; also shown in *Leise et al. (2012, Fig. 6(b))*) has the main features predicted by our theory, namely a peak at zero frequency, a dominant peak at the circadian frequency and a second harmonic. We therefore investigate if the experimental data can be fit by our proposed theoretical expression for the power spectrum, Eq. (20). Our strategy is as follows: (i) we propose a biologically plausible network motif explaining the observed oscillatory single cell dynamics, (ii) we fit the principal peak of the experimental power spectrum using the LNA for this motif and (iii) we refine our fit by taking into account the additional peaks in the spectrum using our main result, Eq. (20), applied to the motif.

The ability of biological systems to oscillate is often associated with the presence of a negative feedback loop in the underlying biochemical network (*Novák and Tyson, 2008*). Given the fact that any biochemical oscillator must be composed of at least three components we propose a negative feedback motif involving mRNA (*M*) and two forms of a protein (*P* and *P**) as a candidate for explaining the experimental rhythmic fibroblast data (see Fig. 3 (a) for an illustration). The dynamics for this motif could for example be deterministically described by the set of coupled rate equations

$$\partial_t \phi_M = \frac{k_0}{k_1 + \phi_P} - \alpha_1 \phi_M, \tag{24}$$

$$\partial_t \phi_{P^*} = \beta_1 \phi_M - \alpha_2 \phi_{P^*}, \tag{25}$$

$$\partial_t \phi_P = \beta_2 \phi_{P^*} - \frac{k_2 \phi_P}{k_3 + \phi_P}, \tag{26}$$

where ϕ_M , ϕ_{P^*} and ϕ_P are the concentrations of mRNA and the two proteins. The Jacobian for these rate equations is given by

$$\underline{J} = \begin{pmatrix} -\alpha_1 & 0 & -\chi \\ \beta_1 & -\alpha_2 & 0 \\ 0 & \beta_2 & -\alpha_3 \end{pmatrix}, \tag{27}$$

where $\alpha_{1,2,3}$, $\beta_{1,2}$ and χ are positive constants. Note that χ measures the strength of the negative feedback loop and is equal to $k_0/(k_1 + \phi_P)^2$ whereas α_3 is a measure of the nonlinear protein

degradation rate and is equal to $k_2 k_3 / (k_3 + \phi_P)^2$. Indeed it can be shown that this is a generic form for the Jacobian of all negative feedback motifs with three components (*Tyson, 2002*). The only entries of the Jacobian which are functions of a concentration are J_{13} and J_{33} which are functions of ϕ_P , the concentration of protein. Hence the only non-zero Hessian elements are J_1^{33} and J_3^{33} ; this is since we assumed that feedback repression and protein degradation steps occur via bimolecular (nonlinear) mechanisms. The Routh–Hurwitz theorem implies that the steady state is stable provided $(\alpha_1 + \alpha_2 + \alpha_3)(\alpha_1 \alpha_2 + \alpha_2 \alpha_3 + \alpha_3 \alpha_1) > \alpha_1 \alpha_2 \alpha_3 + \beta_1 \beta_2 \chi$. If equality holds the system undergoes a Hopf bifurcation. Close to the bifurcation the system has a pair of complex conjugate eigenvalues with dominant imaginary part which can be approximated by $\omega_0 \approx \sqrt{\alpha_1 \alpha_2 + \alpha_2 \alpha_3 + \alpha_3 \alpha_1}$; this determines the frequency of the principal peak of the power spectrum of the negative feedback loop close to the bifurcation.

We now use the functional form of the LNA power spectrum, Eq. (8) together with Eq. (27), to obtain a fit of the protein species *P*s spectrum to the principal peak of the experimental power spectrum. Since our proposed oscillator is composed of three components but the available experimental data is for only one of these components, we reduce the number of free parameters to fit the LNA by setting $\alpha_{1,2} = \beta_{1,2}$ and assuming the noise matrix \underline{BB}^T is proportional to the unit matrix, i.e., a total of four free parameters since the Jacobian has three parameters and the diagonal noise matrix has one parameter. We then use a least squares nonlinear fitting procedure to obtain these four parameters; the result is shown as a gray dashed line in Fig. 3(b) where the parameters are $\alpha_{1,2} = \beta_{1,2} = 0.51$, $\alpha_3 = 0.82$, $\chi = 5.99$ and $\Omega^{-1}[\underline{BB}^T]_{11} = \Omega^{-1}[\underline{BB}^T]_{22} = \Omega^{-1}[\underline{BB}^T]_{33} = 0.01$. The solid blue line in Fig. 3(b) shows the power spectrum reproduced from the experimental dataset obtained by *Leise et al. (2012)*.

We next refined our fit by using Eq. (20) in the previous section. To compute this we need the two parameters determining the critical eigenmodes of the Jacobian (γ and ω_0), the noise coefficient G/Ω , the matrix \underline{U} of eigenvectors of the Jacobian and the Hessian. All of the latter except for the Hessian can be computed from the four free parameters previously determined by fitting the LNA spectrum since these completely determine the Jacobian and the noise matrix. We use a nonlinear fitting procedure as before to determine the two non-zero components of the Hessian matrix and find $J_1^{33} = 16.20$ and $J_3^{33} = 2.23$. The spectrum given by Eq. (20) and using the total of six parameter values determined by the fitting procedure is shown as a magenta line in Fig. 3(b). The agreement between the experimental data (blue line) and our theory is remarkable when considering that we required only two additional parameters to fit the two new features predicted by our

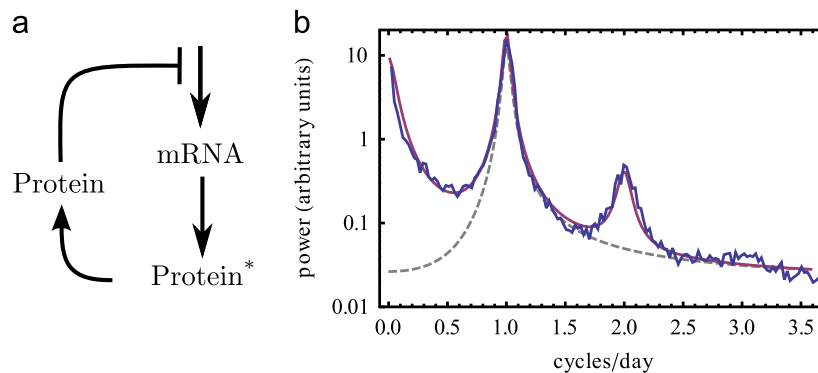


Fig. 3. Least squares fit of the experimental power spectrum of circadian rhythm in fibroblast cells by the LNA and our nonlinear theory. (a) A biologically plausible motif for explaining the single cell dynamics observed in *Leise et al. (2012)*. (b) Fit of the experimental power spectrum (solid blue line) by the linear (LNA) theory (gray dashed line) and by the proposed nonlinear theory (magenta solid line) is shown. Note that the LNA captures well the principal peak while it misses the appearance of the peaks at zero and at a second harmonic frequency. The nonlinear theory is in excellent quantitative agreement with all features of the experimental data. The parameters for the theoretical curves are given in the main text. (For interpretation of the references to color in this figure caption, the reader is referred to the web version of this article.)

theory, namely the peak at zero frequency and the second order harmonic. Subtracting a constant background of 0.001% of the central peak height from the experimental spectrum improved the agreement, presumably because this eliminates measurement noise which our theory does not describe.

We shall next consider two theoretical models of biochemical relevance and show in detail how one calculates the analytical power spectrum Eq. (20) for these systems. We also verify all our predictions by detailed stochastic simulations using the SSA.

4.2. Oscillator control of mitosis

Here we investigate the effect of NIOs on a simple model proposed by Tyson and Kauffman (1975) for the control of the mitotic phase of the cell cycle



where the species X and Y are the forms of inactive and active proteins, respectively. In the following we give a detailed step-by-step derivation how the power spectrum given by Eq. (20) is obtained for the model under consideration. For the above set of reactions, the state-change vectors are given by

$$\mu_1 = (1, 0)^T, \quad \mu_2 = (-1, 1)^T, \quad \mu_3 = (0, -1)^T, \quad \mu_4 = (-1, 1)^T, \quad (29)$$

where the first and second entries in these vectors represent the change in the number of X and Y molecules for each reaction, respectively. Note that the reactions are here numbered from 1 to 4, where the order follows that in which they appear in (28). The associated propensities are

$$a(\mu_1, \mathbf{x}\Omega) = \Omega k, \quad a(\mu_2, \mathbf{x}\Omega) = \Omega bx, \quad a(\mu_3, \mathbf{x}\Omega) = \Omega y, \quad a(\mu_4, \mathbf{x}\Omega) = \Omega y^2 x. \quad (30)$$

We have here used x and y to denote the number of molecules per unit volume of the respective species. The constants k and b denote the rate constants of the first and second reaction in (28), respectively, while the remaining reactions are assumed to occur with unit rate. Note also that the last propensity has been approximated by its large concentration limit, namely the same limit by which the CLE is valid. The corresponding CLE for this set of reaction is then given by

$$\frac{d}{dt} x = k - bx - y^2 x + \Omega^{-1/2} (\sqrt{k}\Gamma_1(t) - \sqrt{bx}\Gamma_2(t) - \sqrt{y^2 x}\Gamma_4(t)), \quad (31a)$$

$$\frac{d}{dt} y = bx + y^2 x - y + \Omega^{-1/2} (\sqrt{bx}\Gamma_2(t) - \sqrt{y}\Gamma_3(t) + \sqrt{y^2 x}\Gamma_4(t)). \quad (31b)$$

The analysis will be carried out in two steps: first we work out the power spectrum within the LNA and next we compute the novel higher-order corrections. An inspection of Eq. (8) shows that to calculate the LNA, we need the Jacobian of the REs, \underline{J} , and the noise matrix, \underline{B} . The REs are obtained from the nonlinear Langevin equations (31) above by taking the limit $\Omega \rightarrow \infty$. These are found to have a steady state solution $\phi_X = k/(k^2 + b)$ and $\phi_Y = k$. We make the following convenient definitions: $k = 2^{-1/2} \omega_0 (1 + \omega_0^2)^{1/2}$ and $b = (\theta^2 + \gamma - k^2)$ where $\theta^2 = (\sqrt{4\gamma(\gamma-1)} + (1 + 2\omega_0^2)^2 - 1)/2$; it then follows that at steady state we can write the Jacobian as

$$\underline{J} = \begin{pmatrix} -\gamma - \theta^2 & \gamma - 1 - \theta^2 \\ \gamma + \theta^2 & -\gamma + \theta^2 \end{pmatrix}, \quad (32)$$

whose eigenvalues can be found analytically as in Tyson and Kauffman (1975) and are given by

$$\lambda_{1,2} = -\gamma \pm i\sqrt{\gamma(1-\gamma) + \theta^2}. \quad (33)$$

We observe that the Hopf bifurcation is approached as $\gamma \rightarrow 0$ with $\omega_0 = \lim_{\gamma \rightarrow 0} \theta$ being the NIO frequency. We next systematically approximate the inverse $(\underline{J} - i\omega)^{-1}$ which becomes singular at ω_0 as the bifurcation is approached and hence has to be handled with extra care. Therefore using the Jacobian in Eq. (32) we write

$$(\underline{J} - i\omega)^{-1} = C^{-1}(\omega) \begin{pmatrix} \omega_0^2 - i\omega & 1 + \omega_0^2 \\ -\omega_0^2 & -(\omega_0^2 + i\omega) \end{pmatrix} \quad (34)$$

which is simply the matrix of cofactors of Eq. (32) evaluated at the bifurcation point divided by the full determinant $C(\omega) = \gamma + 2i\gamma\omega + \theta^2 - \omega^2$ of $(\underline{J} - i\omega)$ which denotes the singular part. The noise matrix is computed using the definition after Eq. (12) together with the state-change vectors and propensities given by Eqs. (29) and (30), respectively, and substituting the steady state concentrations. The result after taking the limit $\gamma \rightarrow 0$ is given by

$$\underline{B}\underline{B}^T = \omega_0 \sqrt{2(1 + \omega_0^2)} \begin{pmatrix} 1 & -\frac{1}{2} \\ -\frac{1}{2} & 1 \end{pmatrix}. \quad (35)$$

Using Eq. (8) together with Eqs. (34) and (35) the LNA power spectra can be expressed as

$$P_X^{\text{LNA}}(\omega) = \frac{1}{\Omega} \frac{\omega_0 \sqrt{2(1 + \omega_0^2)} (1 + \omega^2 + \omega_0^2 + \omega_0^4)}{(\gamma + \theta^2 - \omega^2)^2 + (2\gamma\omega)^2}, \quad (36a)$$

$$P_Y^{\text{LNA}}(\omega) = \frac{1}{\Omega} \frac{\omega_0 \sqrt{2(1 + \omega_0^2)} (\omega^2 + \omega_0^4)}{(\gamma + \theta^2 - \omega^2)^2 + (2\gamma\omega)^2}, \quad (36b)$$

which have a resonance at $\omega = \omega_0$ in both variables due to the dependence of the denominator.

Next we calculate the corrections accounting for nonlinear effects close to the bifurcation; an inspection of Eq. (20) shows that we need to compute the Hessian of the REs and the matrix of eigenvectors of the Jacobian. The former is obtained by differentiating the right hand side of the rate equations (the nonlinear Langevin equations (31) with $\Omega \rightarrow \infty$) twice and substituting the steady state concentrations

$$\left(\frac{\partial^2 f_2(\phi)}{\partial \alpha \partial \beta} \right) = - \left(\frac{\partial^2 f_1(\phi)}{\partial \alpha \partial \beta} \right) = \omega_0 \sqrt{2(1 + \omega_0^2)} \begin{pmatrix} 0 & 1 \\ 1 & (\gamma + \theta^2)^{-1} \end{pmatrix}, \quad (37)$$

where $\partial^2 f_1 / (\partial \alpha \partial \beta)$ is the Hessian of the deterministic equation for x , $\partial^2 f_2 / (\partial \alpha \partial \beta)$ is the Hessian for the corresponding equation for y where α and β can be either x or y .

Using the eigenvalues, Eq. (33), and the Jacobian Eq. (32), we can compute \underline{U} by means of the definition after Eq. (9) and obtain in the limit $\gamma \rightarrow 0$

$$\underline{U} = \begin{pmatrix} \omega_0 & i + \omega_0 \\ \omega_0 & -i + \omega_0 \end{pmatrix}. \quad (38)$$

Using Eq. (38) together with Eq. (35) we find

$$\underline{B}\underline{B}^T = \omega_0 \sqrt{2(1 + \omega_0^2)} \begin{pmatrix} 1 + \omega_0^2 & \omega_0^2 - 1 + i\omega_0 \\ \omega_0^2 - 1 - i\omega_0 & 1 + \omega_0^2 \end{pmatrix}, \quad (39)$$

and hence we have $G = [\underline{B}\underline{B}^T]_{11} = [\underline{B}\underline{B}^T]_{22} = \sqrt{2}\omega_0(1 + \omega_0^2)^{3/2}$. Substituting Eqs. (34), (37), (38) into Eq. (21) and taking the limit $\gamma \rightarrow 0$, we obtain the Hessian coefficients in the eigenrepresentation:

$$M_1^{11}(\omega) = C^{-1}(\omega) \frac{(1 + i\omega) \sqrt{1 + \omega_0^2} (2\omega_0^2 - 2i\omega_0 - 1)}{2\sqrt{2}\omega_0}, \quad (40a)$$

$$M_1^{12}(\omega) = C^{-1}(\omega) \frac{(1 + i\omega) \sqrt{1 + \omega_0^2} (1 - 2\omega_0^2)}{2\sqrt{2}\omega_0}, \quad (40b)$$

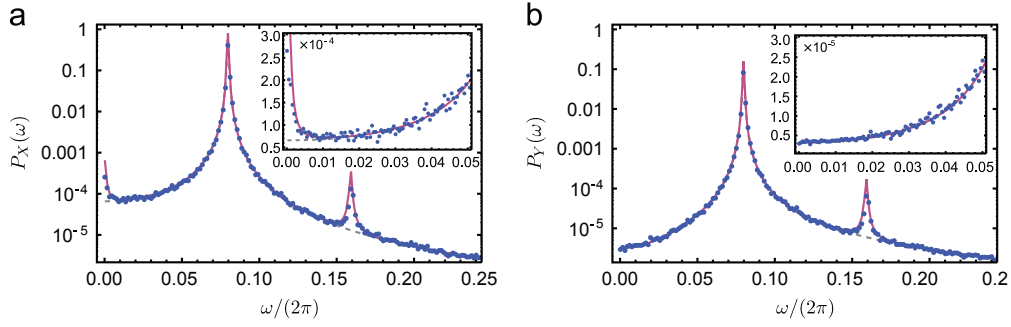


Fig. 4. Noise-induced oscillations in the mitosis control mechanism (28). We compare the predictions of our theory of the power spectra, Eqs. (41) (solid magenta line) to those obtained from stochastic simulations using the SSA (blue dots) for the inactive X and active protein Y as shown in (a) and (b), respectively. Note that our theory accurately predicts the peak at the zero frequency in (a) (see also the inset for a magnified view) and the peaks at twice the fundamental frequency in (a) and (b) which are missed by the power spectra predicted by the LNA (gray dashed line). The parameters used are $k=0.3953$, $b=0.0946$ and $\Omega=2.5 \times 10^5$ which yield $\gamma=0.0025$ and $\omega_0=0.5$. (For interpretation of the references to color in this figure caption, the reader is referred to the web version of this article.)

$$M_2^{11}(\omega) = C^{-1}(\omega) \frac{i\omega(1 + 2i\omega_0 - 2\omega_0^2)\sqrt{1 + \omega_0^2}}{2\sqrt{2}\omega_0}, \quad (40c)$$

$$M_2^{12}(\omega) = C^{-1}(\omega) \frac{i\omega\sqrt{1 + \omega_0^2}(2\omega_0^2 - 1)}{2\sqrt{2}\omega_0}. \quad (40d)$$

Note that $C(\omega)$ is given by the determinant after Eq. (34). Finally substituting these coefficients and G (given after Eq. (39)) into Eq. (20), we find the corrections to the LNA spectrum of fluctuations

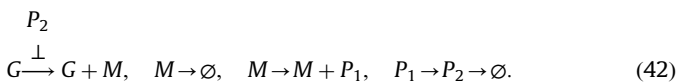
$$P_X(\omega) = P_X^{\text{LNA}}(\omega) + \frac{\Omega^{-2}}{8\gamma} \frac{(1 + \omega^2)(1 + \omega_0^2)^3}{(\gamma + \theta^2 - \omega^2)^2 + (2\gamma\omega)^2} \left(\frac{1 + (\omega_0 + 2\omega_0^2)^2}{(\omega - 2\omega_0)^2 + (2\gamma)^2} + \frac{2 - 6\omega_0^2 + 8\omega_0^4}{\omega^2 + (2\gamma)^2} \right), \quad (41a)$$

$$P_Y(\omega) = P_Y^{\text{LNA}}(\omega) + \frac{\Omega^{-2}}{8\gamma} \frac{\omega^2(1 + \omega_0^2)^3}{(\gamma + \theta^2 - \omega^2)^2 + (2\gamma\omega)^2} \left(\frac{1 + (\omega_0 + 2\omega_0^2)^2}{(\omega - 2\omega_0)^2 + (2\gamma)^2} + \frac{2 - 6\omega_0^2 + 8\omega_0^4}{\omega^2 + (2\gamma)^2} \right). \quad (41b)$$

From the form of Eqs. (41) one can deduce that the theory predicts a second harmonic peak for both species but only a peak at zero frequency in the spectrum of species X (compare Fig. 4(a) and (b)). The good quantitative agreement between theory and simulations verifies the accuracy of the proposed novel theory.

4.3. Genetic oscillator with transcriptional feedback

Finally, we demonstrate the nonlinearity induced effects for the modified Goodwin model involving non-elementary reactions (Tyson, 2002; Bliss et al., 1982). This model is based on a negative loop and is widely used to describe many transcriptional oscillators such as circadian clocks (Roenneberg et al., 2008). The model comprises three chemical constituents M , P_1 and P_2 denoting mRNA, cytosolic and nuclear protein species, respectively. Schematically, such reaction network may be represented as



From the above reaction scheme, one can construct the state-change vectors

$$\mu_1 = (1, 0, 0), \quad \mu_2 = (-1, 0, 0), \quad \mu_3 = (0, 1, 0), \quad \mu_4 = (0, -1, 1), \quad \mu_5 = (0, 0, -1), \quad (43)$$

where the first, second and third entries in these vectors represent the change in the number of M , P_1 and P_2 molecules for each reaction, respectively. Note that the reactions are here numbered from 1 to 5, where the order follows that in which they appear in (42). The

associated propensities are $a(\mu_1, \mathbf{x}\Omega) = \Omega k / (1 + x_{P_2})$, $a(\mu_2, \mathbf{x}\Omega) = \Omega b x_M$, $a(\mu_3, \mathbf{x}\Omega) = \Omega b x_M$, $a(\mu_4, \mathbf{x}\Omega) = \Omega b x_{P_1}$, and $a(\mu_5, \mathbf{x}\Omega) = \Omega c x_{P_2} / (1 + x_{P_2})$. We have here used x_M, x_{P_1}, x_{P_2} to denote the number of molecules per unit volume of the respective species. Note that the repression and protein degradation steps (first and last reactions) are modeled by non-elementary reactions. The constant k gives the mRNA production rate in the absence of repression, c is the rate of enzymatic degradation of protein P_2 at low protein concentrations while the remaining first-order reactions in (42) are assumed to occur with rate b . The CLE for this system is given by

$$\frac{d}{dt} x_M = \frac{k}{1 + x_{P_2}} - b x_M + \Omega^{-1/2} \left(\sqrt{\frac{k}{1 + x_{P_2}}} \Gamma_1(t) - \sqrt{b x_M} \Gamma_2(t) \right), \quad (44a)$$

$$\frac{d}{dt} x_{P_1} = b x_M - b x_{P_1} + \Omega^{-1/2} (\sqrt{b x_M} \Gamma_3(t) - \sqrt{b x_{P_1}} \Gamma_4(t)), \quad (44b)$$

$$\frac{d}{dt} x_{P_2} = b x_{P_1} - \frac{c x_{P_2}}{1 + x_{P_2}} + \Omega^{-1/2} \left(\sqrt{b x_{P_1}} \Gamma_4(t) - \sqrt{\frac{c x_{P_2}}{1 + x_{P_2}}} \Gamma_5(t) \right). \quad (44c)$$

The analysis proceeds as in the previous example; one first obtains the power spectrum within the LNA and then calculates the corrections to the spectrum using the proposed theory. Both of these can be computed from the state-change vectors and propensities given in the beginning of this section and following the same steps as in the previous example. We make a further simplifying assumption to make the analysis more tractable: we assume that $c > b$ and that $k = c(\sqrt{c/b} - 1)$. It can then be shown that to the LNA level of approximation, the power spectrum of mRNA and protein species is given by

$$P_M^{\text{LNA}}(\omega) = \frac{16\omega_0(3\omega^2 + \omega_0^2)(3\omega^2 + 65\omega_0^2)}{\sqrt{3}\Omega|C(\omega)|^2}, \quad (45a)$$

$$P_{P_1}^{\text{LNA}}(\omega) = \frac{16\omega_0(9\omega^4 - 15\omega^2\omega_0^2 + 74\omega_0^4)}{\sqrt{3}\Omega|C(\omega)|^2}, \quad (45b)$$

$$P_{P_2}^{\text{LNA}}(\omega) = \frac{16\omega_0(9\omega^4 + 6\omega^2\omega_0^2 + 2\omega_0^4)}{\sqrt{3}\Omega|C(\omega)|^2}, \quad (45c)$$

where $C(\omega) = (2\gamma - \sqrt{3}\omega_0 - i\omega)(\omega_0^2 - \omega^2 - 2\sqrt{3}\omega_0\gamma + 4\gamma^2 + 2i\gamma\omega)$ with $\omega_0 = \sqrt{3}b$ and $\gamma = b(1 - (\sqrt{c/b} - 1)^{1/3})/2$. The form of $C(\omega)$ implies that the power spectra have a peak at $\omega \approx \omega_0$, the size of which increases with decreasing γ . Thus the rate constant b controls the frequency of the NIOs whereas the ratio of the rate constants c/b controls how close is the system to the Hopf bifurcation and hence the quality of the oscillations.

According to our theory, Eq. (20), the power spectra corrected for nonlinear effects are given by

$$P_M(\omega) = P_M^{\text{LNA}}(\omega) + \frac{36992}{2187\Omega^2} \frac{\omega_0^4 \omega^2 (\omega_0^2 + 3\omega^2)}{\gamma |C(\omega)|^2} \left(\frac{1}{(\omega - 2\omega_0)^2 + (2\gamma)^2} + \frac{2}{\omega^2 + (2\gamma)^2} \right), \quad (46a)$$

$$P_{P_1}(\omega) = P_{P_1}^{\text{LNA}}(\omega) + \frac{36992}{2187\Omega^2} \frac{\omega_0^6 \omega^2}{\gamma |C(\omega)|^2} \left(\frac{1}{(\omega - 2\omega_0)^2 + (2\gamma)^2} + \frac{2}{\omega^2 + (2\gamma)^2} \right), \quad (46b)$$

$$P_{P_2}(\omega) = P_{P_2}^{\text{LNA}}(\omega) + \frac{578}{2187\Omega^2} \frac{\omega_0^4 (27\omega_0^4 - 14\omega_0^2 \omega^2 + 3\omega^4)}{\gamma |C(\omega)|^2} \left(\frac{1}{(\omega - 2\omega_0)^2 + (2\gamma)^2} + \frac{2}{\omega^2 + (2\gamma)^2} \right). \quad (46c)$$

In Fig. 5, we compare the theoretical spectra obtained from our theory and the LNA with spectra obtained from stochastic simulations using the SSA for three different values of the volume

Ω . Our theory is in excellent agreement with simulations for the largest volume (see Fig. 5(a) and (b)); the corresponding LNA prediction is also in good agreement except for ω close to zero. The spectra at intermediate volumes are in very good quantitative agreement with those from the proposed theory whereas the LNA misses the main features (see Fig. 5(c) and (d)). In particular we see that the simulations verify the predictions given by Eqs. (46a)–(46c) namely that the corrections to the LNA spectra exhibit a second harmonic for all three species, however, an additional peak at zero frequency is only predicted for protein P_2 . The simulation data shows two contrasting types of phenomena as the volume is decreased further: (i) for the mRNA spectrum, in addition to the second harmonic, a third-order harmonic becomes conspicuous and (ii) for the protein spectrum, the second harmonic which was visible at intermediate volumes disappears (see Fig. 5(e) and (f)). Both of these phenomena cannot be explained by the present theory, but rather come within the scope of the next higher-order corrections to the LNA (order Ω^{-3}).

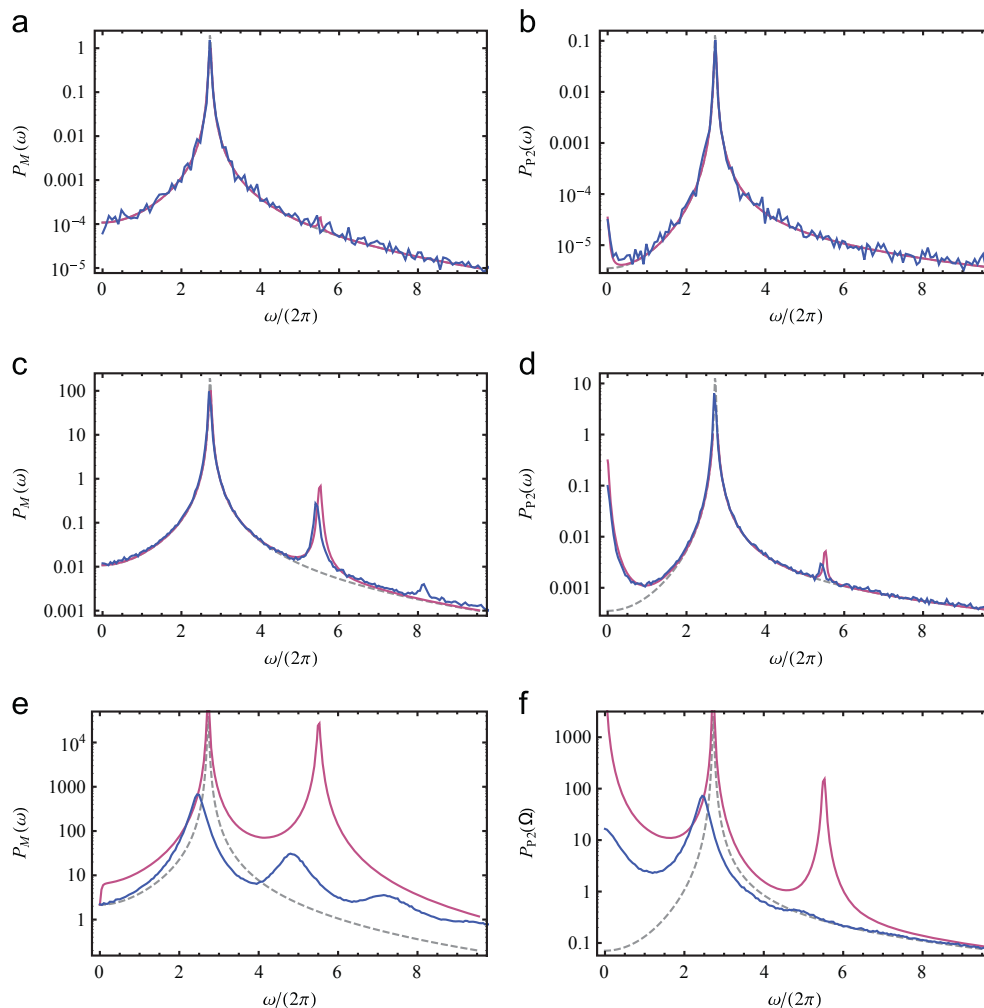


Fig. 5. Noise-induced oscillations of a negative feedback loop, see mechanism (42). We compare the power spectra of species M and P_2 for three different volumes which have been obtained from the analytic theory (solid magenta line), i.e., using Eqs. (46a) and (46c), and from stochastic simulations using the SSA (blue line). For comparison we also plot the LNA (dashed gray line). Panels (a) and (b) show that the simulation power spectra for large volumes ($\Omega = 1 \times 10^5$) are in good agreement with the LNA except at zero frequency (dashed lines) as well with the predictions of our theory. For intermediate volumes ($\Omega = 1000$) both spectra show a peak at the second harmonic as well as a zero frequency peak in the protein power spectrum (panels (c) and (d)). The latter peaks are well reproduced by our theory. For very small volumes ($\Omega = 5$) as shown in panels (e) and (f), our theory predicts the existence of a second harmonic in the mRNA concentration and a zero frequency peak in the protein concentration but misses the attenuation of the second harmonic and the amplification of a third harmonic in protein and mRNA spectra, respectively. In this case neither the proposed theory nor the LNA matches the frequency dependence of the power spectrum very well. In all panels we have used the parameter values $c=765$, $b=10$ yielding $\gamma=0.1$ and $\omega_0/(2\pi)=2.8$: (a) $\Omega=10^5$; (b) $\Omega=10^5$; (c) $\Omega=10^3$; (d) $\Omega=10^3$; (e) $\Omega=5$; and (f) $\Omega=5$. (For interpretation of the references to color in this figure caption, the reader is referred to the web version of this article.)

5. Discussion

In summary, we have developed a nonlinear theory of NIOs in biochemical networks. Our analysis is valid in the vicinity of a Hopf bifurcation where the oscillations are most pronounced. We showed that while the linear response (LNA) leads to the principal peak in the spectrum, it is the nonlinear response which accounts for the second harmonic and for the peak at zero frequency. Our results are supported by stochastic simulations using the SSA of mitotic and Goodwin oscillators; the results can also explain rhythmic single cell experimental data which as we have shown cannot be understood within the conventional LNA.

Deriving explicit analytical expressions for the power spectra of NIOs is desirable for various reasons: (i) to deduce the existence of NIOs, (ii) to study the parametric dependence of the NIO quality on the biochemical mechanism, and (iii) to estimate rate constants characterizing biochemical oscillators from single-cell data. While all of these can in principle be obtained from stochastic simulations the procedure is very time-consuming in practice because the large amount of ensemble averaging required to obtain statistically meaningful results.

Our results are of particular importance for understanding the origin of ultradian (12 h) rhythms inside single cells. It has been known that such rhythms accompany circadian (24 h) rhythms (Dowse, 2008), however, their origin is still a matter of debate. We have shown that ultradian rhythms can arise as second harmonics of the circadian oscillation in a population of damped and uncoupled single cell circadian clocks. Our hypothesis is supported by the fact that the average experimental power spectrum of autonomous rhythms in fibroblast cells (Leise et al., 2012) is remarkably well fit by the theoretical spectrum derived from our nonlinear theory.

We note that higher order harmonics have been described early in the theory of small amplitude self-sustained oscillators subject to weak noise (Stratonovich, 1967). The concept of the existence of such harmonics in damped oscillators subject to weak noise is not as intuitive as for self-sustained oscillators since such oscillations do not exist in the absence of noise. Indeed this phenomenon has to date received only scant attention. Previous studies showed the presence of higher order harmonics of NIOs for specific models by means of simulations (Li and Lang, 2008; Rozhnova and Nunes, 2009; Li and Zhu, 2001; Zhong et al., 2001) and a case study through a system size expansion analytic approach (Scott, 2012). Particular progress towards a nonlinear theory of NIOs has recently been obtained using multiple scale analysis for a model of epidemic oscillations in two variables by Chaffee and Kuske (2011). The proposed method separates the dynamics into a fast oscillation (of frequency $\sim \omega_0$) and its slowly varying stochastic amplitude (on a timescale $\sim 1/\gamma$); the same condition is met in the vicinity of a Hopf bifurcation. The exemplary application highlights the emergence of a second harmonic by providing a set of nonlinear SDEs for the amplitudes of the fundamental mode and its higher harmonic. An analytical expression of the power spectrum, however, has not been reported presumably because of the nonlinearity of the resulting equations. Since the method has been applied only to few variable examples it remains unclear how it generalizes to biochemical systems which are typically large (Schwikowski et al., 2000).

Our analysis improves over previous work by deriving for the first time an approximate closed form expression for the power spectrum of NIOs for all monostable biochemical networks operating close to a Hopf bifurcation. This is achieved by calculating an asymptotic expansion of the power spectrum in two parameters: the system size and the distance to the bifurcation point. In particular, our theory shows that the previously observed second harmonic is universally true for all nonlinear damped

biochemical oscillators of arbitrary dimension subject to weak noise. We also derive an explicit condition for the existence of the zero frequency peak in the power spectrum. Note that such a phenomenon is consistent with the ansatz used by Chaffee and Kuske (2011), see also Klosek and Kuske (2005), but has not been explicitly observed for the particular examples studied therein. We show that this phenomenon stems from the fact that the baseline of the oscillation undergoes a Brownian motion on timescales much longer than the period of the oscillations and demonstrate the effect for two biologically relevant models and experimental data of a circadian rhythm in single cells. The biological relevance of this phenomenon is that close to the bifurcation, the baseline of single cell NIOs may vary widely among genetically identical cells and hence is a significant source of cell-to-cell variability.

We conclude by noting that our results show that the conventional linear analysis of biochemical systems using the LNA is limited in scope and that higher-order corrections are important and relevant for understanding and explaining experimental single cell data.

6. Methods

6.1. Linear noise approximation of power spectra

In this section we briefly review the LNA and derive preliminary results which will be useful for the nonlinear analysis in the following section. Within this approximation the mean concentrations as predicted by the CME are equal to those given by the deterministic REs, and the fluctuations about these concentrations are given by a linear SDE of the form

$$\frac{d}{dt} \epsilon(t) = \underline{J}(\phi) \epsilon(t) + \Omega^{-1/2} \underline{B}(\phi) \Gamma(t), \quad (47)$$

where Ω is the volume of the compartment in which the biochemical pathway is confined, and ϵ is a vector of concentration fluctuations about ϕ , the concentration vector solution of the REs, Eq. (2). The remaining quantities are defined after Eq. (7) in the main text.

The linear SDE constitutes what is commonly called the LNA of the CME. Essentially it approximates the trajectories of the CME by those of a multivariate Ornstein–Uhlenbeck process (Gardiner, 2007) which can be solved exactly. Its solution being a multivariate Gaussian distribution and hence all information about the fluctuations are obtained from the knowledge of the correlation matrix $\langle \epsilon(t) \epsilon^T(t + \tau) \rangle \equiv \underline{\Delta}(\tau)$ which can be found analytically from

Eq. (47) as shown in Gardiner (2007). The result is

$$\underline{\Delta}(\tau) = H(\tau) e^{\underline{J} \tau} \underline{\sigma} + H(-\tau) \underline{\sigma} e^{-\underline{J}^T \tau}, \quad (48)$$

where $H(\tau)$ is the Heaviside step function (with $H(0) = 1/2$) and $\underline{\sigma}$ is the covariance matrix satisfying

$$\underline{J} \underline{\sigma} + \underline{\sigma} \underline{J}^T + \underline{B} \underline{B}^T = 0. \quad (49)$$

Note also that $\underline{\sigma}$ equals the correlation matrix $\underline{\Delta}(\tau)$ evaluated at $\tau = 0$. However, the identification of periodicities is not immediately obvious from the matrix equation (48). Therefore we diagonalize the Jacobian by the transformation $\underline{U} \underline{J} \underline{U}^{-1} = \text{diag}(\lambda_1, \lambda_2, \dots, \lambda_N)$. The Langevin equation then becomes

$$\partial_t \tilde{\epsilon}_i(t) = \lambda_i \tilde{\epsilon}_i + \Omega^{-1/2} \sum_{\alpha} \tilde{B}_{i\alpha} \Gamma_{\alpha}(t), \quad (50)$$

where $\tilde{\epsilon}_i(t) = \sum_j U_{ij} \epsilon_j(t)$. The autocorrelation matrix transforms accordingly $\tilde{\underline{\Delta}}(\tau) = \underline{U} \underline{\Delta}(\tau) \underline{U}^{\dagger}$ and its matrix elements read

$$\tilde{\Delta}_{ij}(\tau) = H(\tau) e^{\lambda_i \tau} \tilde{\sigma}_{ij} + H(-\tau) \tilde{\sigma}_{ij} e^{-\lambda_j^* \tau}. \quad (51)$$

From Eq. (49), it can be shown (Elf and Ehrenberg, 2003) that $\tilde{\sigma}_{ij}$ is given by

$$\tilde{\sigma}_{ij} = -\frac{[\tilde{\mathbf{B}}\tilde{\mathbf{B}}^\dagger]_{ij}}{\lambda_i + \lambda_j^*}. \quad (52)$$

Hence, from Eq. (51), we observe that the autocorrelation will exhibit damped oscillations when there is at least one pair of complex conjugate eigenvalues. Using Eqs. (5) and (6), we can write the power spectrum of concentration fluctuations for species s as

$$P_s^{\text{LNA}}(\omega) = \int_{-\infty}^{\infty} e^{-i\omega\tau} \langle \epsilon_s(t)\epsilon_s(t+\tau) \rangle d\tau. \quad (53)$$

The power spectrum can be computed straightforwardly by substituting Eq. (48) in the above equation to obtain (Gardiner, 2007)

$$P_s^{\text{LNA}}(\omega) = \frac{1}{\Omega} [(\underline{\mathbf{J}} - i\omega)^{-1} \underline{\mathbf{B}}\underline{\mathbf{B}}^T (\underline{\mathbf{J}}^T + i\omega)^{-1}]_{ss}. \quad (54)$$

However, such an expression is not particularly useful since the existence of NIOs is not obvious from it. We therefore use the eigenrepresentation to write

$$P_s^{\text{LNA}}(\omega) = \frac{1}{\Omega} \sum_{kl} U_{sk}^{-1} \hat{\Delta}_{kl}(\omega) U_{ls}^{-1}, \quad (55)$$

where $\hat{\Delta}_{kl}(\omega)$ is the Fourier transform of $\tilde{\Delta}_{kl}(\tau)$ which can be computed from Eq. (51) and found to be

$$\hat{\Delta}_{ij}(\omega) = \int_{-\infty}^{\infty} d\tau e^{-i\omega\tau} \tilde{\Delta}_{ij}(\tau) = \frac{[\tilde{\mathbf{B}}\tilde{\mathbf{B}}^\dagger]_{ij}}{(\lambda_i - i\omega)(\lambda_j^* + i\omega)}. \quad (56)$$

where we have used Eq. (51) together with (52). Noting that $\tilde{\mathbf{B}} = \underline{\mathbf{U}}\underline{\mathbf{B}}$ and

$$[(\underline{\mathbf{J}} - i\omega)^{-1}]_{ij} = \sum_k U_{ik}^{-1} (\lambda_k - i\omega)^{-1} U_{kj}, \quad (57)$$

we verify that Eq. (55) together with Eq. (56) is indeed equivalent to Eq. (54).

6.2. Power spectra of nonlinear SDEs

In the main text we have argued that close to the bifurcation point the linear Langevin equation given by the LNA, Eq. (7), is insufficient to capture the dynamics of NIOs and has to be replaced by the following nonlinear Langevin equation in the eigenrepresentation of the Jacobian:

$$\partial_t \tilde{\epsilon}_i(t) = \lambda_i \tilde{\epsilon}_i + \frac{1}{2} \tilde{J}_i^{\alpha\beta}(\boldsymbol{\phi}) \tilde{\epsilon}_\alpha \tilde{\epsilon}_\beta + \Omega^{-1/2} \tilde{B}_{i\alpha}(\boldsymbol{\phi}) \Gamma_\alpha(t), \quad (58)$$

where the tilda denotes variables expressed in the eigenbasis of the Jacobian. Note that, for notational convenience, we have here used the Einstein summation convention where all twice repeated Greek indices are summed over all allowable values; this will be used in the rest of the paper. The above stochastic differential equation differs from the eigenrepresentation of the LNA, Eq. (50), by the second term which takes into account the nonlinearity of the drift and which is important whenever the first term in Eq. (58) is small. Applying the Fourier transform $\tilde{\epsilon}_i(t) = \int (d\omega/2\pi) e^{i\omega t} \hat{\epsilon}_i(\omega)$ to the above equation we find

$$i\omega \hat{\epsilon}_i(\omega) = \lambda_i \hat{\epsilon}_i(\omega) + \Omega^{-1/2} \tilde{B}_{i\alpha} \hat{\Gamma}_\alpha(\omega) + \frac{1}{2} \tilde{J}_i^{\alpha\beta} \int \frac{d\omega'}{2\pi} \int \frac{d\omega''}{2\pi} \delta(\omega - \omega' - \omega'') \hat{\epsilon}_\alpha(\omega') \hat{\epsilon}_\beta(\omega''), \quad (59)$$

where the delta function is defined by $\int (d\omega/2\pi) f(\omega) \delta(\omega) = f(0)$ for any function f . Note also that it is implied that the integration range extends over the full domain $(-\infty, \infty)$ of the integration variables if not otherwise stated. Now we define the spectral matrix of the fluctuations in the eigenrepresentation of the

Jacobian by

$$\tilde{P}_{ij}(\omega) = \langle \hat{\epsilon}_i(\omega) \hat{\epsilon}_j^*(\omega) \rangle - \delta(\omega) \langle \tilde{\epsilon}_i \rangle \langle \tilde{\epsilon}_j \rangle, \quad (60)$$

which is related to the power spectrum of species s by $P_s(\omega) = \sum_{ij} U_{si}^{-1} \tilde{P}_{ij}(\omega) U_{js}^{-1}$. Note that here $\langle \tilde{\epsilon}_i \rangle$ denotes the stationary mean of Eq. (58). An inspection of Eq. (59) shows that it cannot be solved exactly since the two-variable correlation function needed to compute Eq. (60) is coupled to higher order correlators and hence to proceed further an approximation method becomes indispensable.

6.2.1. Expansion of the nonlinear power spectrum

We start by expanding in powers of the inverse square root of the system size

$$\hat{\epsilon}_i = \Omega^{-1/2} \hat{\epsilon}_i^{(0)} + \Omega^{-1} \hat{\epsilon}_i^{(1)} + O(\Omega^{-3/2}). \quad (61)$$

This allows us to write Eq. (60) as the series

$$\begin{aligned} \tilde{P}_{ij}(\omega) = & \Omega^{-1} (\langle \hat{\epsilon}_i^{(0)} \hat{\epsilon}_j^{*(0)} \rangle - \delta(\omega) \langle \hat{\epsilon}_i^{(0)} \rangle \langle \hat{\epsilon}_j^{(0)} \rangle) \\ & + \Omega^{-3/2} (\langle \hat{\epsilon}_i^{(0)} \hat{\epsilon}_j^{*(1)} \rangle - \delta(\omega) \langle \hat{\epsilon}_i^{(0)} \rangle \langle \hat{\epsilon}_j^{(1)} \rangle) \\ & + \Omega^{-3/2} (\langle \hat{\epsilon}_i^{(1)} \hat{\epsilon}_j^{*(0)} \rangle - \delta(\omega) \langle \hat{\epsilon}_i^{(1)} \rangle \langle \hat{\epsilon}_j^{(0)} \rangle) \\ & + \Omega^{-2} (\langle \hat{\epsilon}_i^{(1)} \hat{\epsilon}_j^{*(1)} \rangle - \delta(\omega) \langle \hat{\epsilon}_i^{(1)} \rangle \langle \hat{\epsilon}_j^{(1)} \rangle) + O(\Omega^{-5/2}). \end{aligned} \quad (62)$$

To evaluate these terms we need expressions for $\hat{\epsilon}_i^{(0)}(\omega)$ and $\hat{\epsilon}_i^{(1)}(\omega)$. These can be obtained by substituting Eq. (61) in Eq. (59) and equating terms of order $\Omega^{-1/2}$ and order Ω^{-1} , which leads to the expressions

$$\begin{aligned} (i\omega - \lambda_i) \hat{\epsilon}_i^{(0)}(\omega) &= \tilde{B}_{i\alpha} \hat{\Gamma}_\alpha(\omega), \\ (i\omega - \lambda_i) \hat{\epsilon}_i^{(1)}(\omega) &= \frac{1}{2} \tilde{J}_i^{\alpha\beta} \int \frac{d\omega'}{2\pi} \int \frac{d\omega''}{2\pi} \delta(\omega - \omega' - \omega'') \hat{\epsilon}_\alpha^{(0)}(\omega') \hat{\epsilon}_\beta^{(0)}(\omega''). \end{aligned} \quad (63)$$

By these two equations it is evident that $\langle \hat{\epsilon}_i^{(0)} \rangle = 0$ and $\langle \hat{\epsilon}_i^{(1)} \hat{\epsilon}_j^{*(0)} \rangle = \langle \hat{\epsilon}_i^{(0)} \hat{\epsilon}_j^{*(1)} \rangle = 0$ which follows from the fact that all odd moments of a Gaussian random variable are zero. Hence there remain only two contributions to the power spectrum Eq. (62)

$$\begin{aligned} \tilde{P}_{ij}(\omega) = & \Omega^{-1} \langle \hat{\epsilon}_i^{(0)} \hat{\epsilon}_j^{*(0)} \rangle + \Omega^{-2} (\langle \hat{\epsilon}_i^{(1)} \hat{\epsilon}_j^{*(1)} \rangle - \delta(\omega) \langle \hat{\epsilon}_i^{(1)} \rangle \langle \hat{\epsilon}_j^{(1)} \rangle) \\ & + O(\Omega^{-5/2}). \end{aligned} \quad (64)$$

As we show now, the first term corresponds to the result given by the conventional LNA and the second term is the correction that we are seeking. Using Eq. (63) and

$$\langle \hat{\Gamma}_\alpha(\omega') \hat{\Gamma}_\beta^*(\omega'') \rangle = \int dt' \int dt'' e^{-i\omega't'} e^{i\omega''t''} \langle \Gamma_\alpha(t') \Gamma_\beta(t'') \rangle = \delta_{\alpha\beta} \delta(\omega' - \omega'') \quad (65)$$

it follows that the leading order contribution is given by the LNA result

$$\langle \hat{\epsilon}_i^{(0)}(\omega) \hat{\epsilon}_j^{*(0)}(\omega) \rangle = \hat{\Delta}_{ij}(\omega), \quad (66)$$

in agreement with Eq. (56) in the previous section. Next we analyze the leading order correction to the LNA result, namely the term proportional to Ω^{-2} in Eq. (64). Multiplying the second equation in (63) with its complex conjugate we find

$$\begin{aligned} \langle \hat{\epsilon}_i^{(1)}(\omega) \hat{\epsilon}_j^{*(1)}(\omega) \rangle = & \frac{1}{4D_{ij}(\omega)} \tilde{J}_i^{\alpha\beta} \tilde{J}_j^{\mu\nu} \int \frac{d\omega'}{2\pi} \int \frac{d\omega''}{2\pi} \int \frac{d\omega'''}{2\pi} \delta(\omega - \omega' - \omega'') \\ & \times \delta(\omega - \omega'' - \omega''') \langle \hat{\epsilon}_\alpha^{(0)}(\omega') \hat{\epsilon}_\beta^{(0)}(\omega'') \hat{\epsilon}_\mu^{*(0)}(\omega''') \hat{\epsilon}_\nu^{*(0)}(\omega''') \rangle, \end{aligned} \quad (67)$$

where we have abbreviated the denominator by $D_{ij}(\omega) = (\lambda_i - i\omega)(\lambda_j^* + i\omega)$. The integrand on the right hand side of the above expression is a Gaussian expectation value which can be evaluated using Wick's theorem (Zinn-Justin, 2007). Specifically, the theorem states that the four-point correlation of a centered Gaussian random variable is given by a sum over all pairings of two-point

correlations. The result is

$$\begin{aligned} &\langle \hat{e}_\alpha^{(0)}(\omega') \hat{e}_\beta^{(0)}(\omega'') \hat{e}_\mu^{*(0)}(\omega''') \hat{e}_\nu^{*(0)}(\omega''''') \rangle \\ &= \langle \hat{e}_\alpha^{(0)}(\omega') \hat{e}_\beta^{(0)}(\omega'') \rangle \langle \hat{e}_\mu^{*(0)}(\omega''') \hat{e}_\nu^{*(0)}(\omega''''') \rangle \\ &\quad + \langle \hat{e}_\alpha^{(0)}(\omega') \hat{e}_\mu^{*(0)}(\omega''') \rangle \langle \hat{e}_\beta^{(0)}(\omega'') \hat{e}_\nu^{*(0)}(\omega''''') \rangle \\ &\quad + \langle \hat{e}_\alpha^{(0)}(\omega') \hat{e}_\nu^{*(0)}(\omega''''') \rangle \langle \hat{e}_\beta^{(0)}(\omega'') \hat{e}_\mu^{*(0)}(\omega''') \rangle. \end{aligned} \tag{68}$$

Making use of the stationarity of the process, i.e., $\langle \hat{e}_\alpha^{(0)}(\omega') \hat{e}_\beta^{(0)}(\omega'') \rangle = \langle \hat{e}_\alpha^{(0)}(\omega') \hat{e}_\beta^{(0)}(\omega'') \rangle \delta(\omega' + \omega'')$ and $\langle \hat{e}_\alpha^{(0)}(\omega') \hat{e}_\beta^{*(0)}(\omega'') \rangle = \langle \hat{e}_\alpha^{(0)}(\omega') \hat{e}_\beta^{*(0)}(\omega'') \rangle \delta(\omega' - \omega'')$, we can simplify the above to read

$$\begin{aligned} &\langle \hat{e}_\alpha^{(0)}(\omega') \hat{e}_\beta^{(0)}(\omega'') \hat{e}_\mu^{*(0)}(\omega''') \hat{e}_\nu^{*(0)}(\omega''''') \rangle \\ &= \langle \hat{e}_\alpha^{(0)}(\omega') \hat{e}_\beta^{(0)}(\omega'') \rangle \delta(\omega' + \omega'') \langle \hat{e}_\mu^{*(0)}(\omega''') \hat{e}_\nu^{*(0)}(\omega''''') \rangle \delta(\omega''' + \omega''''') \\ &\quad + \hat{\Delta}_{\alpha\mu}(\omega') \delta(\omega' - \omega''') \hat{\Delta}_{\beta\nu}(\omega'') \delta(\omega'' - \omega''''') \\ &\quad + \hat{\Delta}_{\alpha\nu}(\omega') \delta(\omega' - \omega''''') \hat{\Delta}_{\beta\mu}(\omega'') \delta(\omega'' - \omega'''''). \end{aligned} \tag{69}$$

and hence Eq. (67) is a sum of three terms. By taking the average of Eq. (63) we find that

$$\begin{aligned} \langle \hat{e}_i^{(1)}(\omega) \rangle \langle \hat{e}_j^{*(1)}(\omega) \rangle &= \frac{1}{4D_{ij}(\omega)} \tilde{J}_i^{\alpha\beta} \tilde{J}_j^{*\mu\nu} \int \frac{d\omega'}{2\pi} \int \frac{d\omega''}{2\pi} \delta(\omega - \omega' - \omega'') \langle \hat{e}_\alpha^{(0)}(\omega') \hat{e}_\beta^{(0)}(\omega'') \rangle \delta(\omega' + \omega'') \\ &\quad \times \int \frac{d\omega'''}{2\pi} \int \frac{d\omega''''}{2\pi} \delta(\omega - \omega''' - \omega''''') \langle \hat{e}_\mu^{*(0)}(\omega''') \hat{e}_\nu^{*(0)}(\omega''''') \rangle \delta(\omega''' + \omega'''''). \end{aligned} \tag{70}$$

Using the above expression together with Eq. (69) in Eq. (67) and simplifying we obtain

$$\begin{aligned} &\langle \hat{e}_i^{(1)}(\omega) \hat{e}_j^{*(1)}(\omega) \rangle - \langle \hat{e}_i^{(1)}(\omega) \rangle \langle \hat{e}_j^{*(1)}(\omega) \rangle \\ &= \frac{1}{2D_{ij}(\omega)} \tilde{J}_i^{\alpha\beta} \tilde{J}_j^{*\mu\nu} \int \frac{d\omega'}{2\pi} \int \frac{d\omega''}{2\pi} \delta(\omega - \omega' - \omega'') \hat{\Delta}_{\alpha\mu}(\omega') \hat{\Delta}_{\beta\nu}(\omega'') \\ &= \frac{1}{2D_{ij}(\omega)} \tilde{J}_i^{\alpha\beta} \tilde{J}_j^{*\mu\nu} \int \frac{d\omega''}{2\pi} \hat{\Delta}_{\alpha\mu}(\omega - \omega'') \hat{\Delta}_{\beta\nu}(\omega''). \end{aligned} \tag{71}$$

Note that by the symmetry $\tilde{J}_i^{\alpha\beta} = \tilde{J}_i^{\beta\alpha}$ the last two terms of Eq. (69) give equal contributions to Eq. (71). Inserting the Fourier transform $\hat{\Delta}_{ij}(\omega) = \int d\tau e^{-i\omega\tau} \tilde{\Delta}_{ij}(\tau)$ we find the spectral matrix expressed as the Fourier integral

$$\tilde{P}_{ij}(\omega) = \Omega^{-1} \hat{\Delta}_{ij}(\omega) + \frac{\Omega^{-2}}{2D_{ij}(\omega)} \tilde{J}_i^{\alpha\beta} \tilde{J}_j^{*\mu\nu} \int_{-\infty}^{\infty} d\tau e^{-i\omega\tau} \tilde{\Delta}_{\alpha\mu}(\tau) \tilde{\Delta}_{\beta\nu}(\tau), \tag{72}$$

which can be carried out analytically. Substituting the LNA auto-correlation matrix given by Eq. (51) we find

$$\begin{aligned} &\int_{-\infty}^{\infty} d\tau e^{-i\omega\tau} \tilde{\Delta}_{\alpha\mu}(\tau) \tilde{\Delta}_{\beta\nu}(\tau) \\ &= \tilde{\sigma}_{\alpha\mu} \tilde{\sigma}_{\beta\nu} \left(\int_0^{\infty} d\tau e^{-i\omega\tau} e^{(\lambda_\alpha + \lambda_\beta)\tau} + \int_{-\infty}^0 d\tau e^{-i\omega\tau} e^{-(\lambda_\mu^* + \lambda_\nu^*)\tau} \right) \\ &= -\tilde{\sigma}_{\alpha\mu} \tilde{\sigma}_{\beta\nu}^* \left(\frac{1}{\lambda_\alpha + \lambda_\beta - i\omega} + \frac{1}{\lambda_\mu^* + \lambda_\nu^* + i\omega} \right). \end{aligned} \tag{73}$$

Substituting the above result into Eq. (72) we conclude that the power spectrum of the nonlinear Langevin Eq. (58) is given by

$$\tilde{P}_{ij}(\omega) = \Omega^{-1} \hat{\Delta}_{ij}(\omega) - \frac{\Omega^{-2}}{2D_{ij}(\omega)} \tilde{J}_i^{\alpha\beta} \tilde{\sigma}_{\alpha\mu} \left(\frac{1}{\lambda_\alpha + \lambda_\beta - i\omega} + \frac{1}{\lambda_\mu^* + \lambda_\nu^* + i\omega} \right) \tilde{J}_j^{*\mu\nu} \tilde{\sigma}_{\beta\nu}^* + O(\Omega^{-5/2}), \tag{74}$$

which has been expressed in the eigenrepresentation of the Jacobian.

6.2.2. Dependence close to the Hopf bifurcation point

The result of the preceding section, as we have argued, approximates the CME in the limit of large population numbers close to the Hopf bifurcation point. The correction term beyond leading order is given by a sum weighted by the eigenmode

covariance $\tilde{\sigma}_{ij}$ and can be simplified by taking into account the dependence on the bifurcation parameter γ . Using the critical eigenvalues $\lambda_{1,2} = -\gamma \pm i\omega_0$ in Eq. (52) we see that the components belonging to the critical modes become singular at the critical point, i.e., $\tilde{\sigma}_{ij} \approx \delta_{ij} G / (2\gamma) + O(\gamma^0)$ (for i and j equal to 1 or 2) and hence yield the major contribution to the sum. Here we have introduced the real quantity G given by

$$G \equiv [\tilde{B}\tilde{B}^\dagger]_{11} = [\tilde{B}\tilde{B}^\dagger]_{22} \tag{75}$$

when the critical eigenvectors are normalized such that $U_{1\alpha} = U_{2\alpha}^*$. We then have

$$\begin{aligned} \tilde{P}_{ij}(\omega) &= \Omega^{-1} \hat{\Delta}_{ij}(\omega) + \frac{\Omega^{-2} G^2}{2\gamma D_{ij}(\omega)} \sum_{\alpha, \beta \in \{1,2\}} \frac{\tilde{J}_i^{\alpha\beta} \tilde{J}_j^{*\alpha\beta}}{|\lambda_\alpha + \lambda_\beta - i\omega|^2} + O(\gamma^0) \\ &\quad + O(\Omega^{-5/2}). \end{aligned} \tag{76}$$

Making use of relation (57) we can define the coefficients $M_s^{kl}(\omega) = [(\mathbb{1} - i\omega)^{-1}]_{s\alpha} U_{\mu k}^{-1} U_{\nu l}^{-1} (\partial^2 f_\alpha(\phi) / \partial \phi_\mu \partial \phi_\nu)$ which given $U_{\bar{1}}^{-1} = U_{\bar{2}}^{-1*}$ have the symmetries $M_s^{11}(\omega) = M_s^{*22}(-\omega)$ and $M_s^{12}(\omega) = M_s^{21}(\omega)$. Using these together with Eq. (76) we can express the power spectrum of concentration fluctuations of species s close to the Hopf bifurcation

$$P_s(\omega) = \sum_{ij} U_{s\bar{i}}^{-1} \tilde{P}_{ij} U_{j\bar{s}}^\dagger \tag{77}$$

$$r(\omega) = P_s^{\text{LNA}}(\omega) + \frac{\Omega^{-2} G^2}{2\gamma} \sum_{\alpha, \beta \in \{1,2\}} \frac{|M_s^{\alpha\beta}(\omega)|^2}{|\lambda_\alpha + \lambda_\beta - i\omega|^2} + O(\Omega^{-5/2}) + O(\gamma^0). \tag{78}$$

Note that the first term is the prediction of the LNA of order Ω^{-1} which as previously discussed leads to a peak at $\omega \approx \omega_0$. The Ω^{-2} correction to the LNA can be understood using the explicit form of the eigenvalues $\lambda_{1,2}$ and expanding the denominator as

$$\begin{aligned} P_s(\omega) &= P_s^{\text{LNA}}(\omega) + \frac{\Omega^{-2} G^2}{2\gamma} \left(\frac{|M_s^{11}(\omega)|^2}{(2\gamma)^2 + (2\omega_0 - \omega)^2} + 2 \frac{|M_s^{12}(\omega)|^2}{(2\gamma)^2 + \omega^2} + \frac{|M_s^{22}(\omega)|^2}{(2\gamma)^2 + (2\omega_0 + \omega)^2} \right) \\ &\quad + O(\Omega^{-5/2}) + O(\gamma^0). \end{aligned} \tag{79}$$

This implies that the first two terms of the corrections yield a peak at twice the frequency of the LNA and another peak at zero frequency whenever γ is small which is our central result. Note that the last term is a non-resonant contribution which has been omitted in our main result, Eq. (20).

Acknowledgments

P.T. and R.G. acknowledge support from FRIAS (Freiburg Institute for Advanced Studies) during their stay in Freiburg in 2011, where most of the research was done. C.F. acknowledges support by the BMBF – Freiburg Initiative in Systems Biology Grant 031392 (FRISYS).

References

Allen, E.J., Allen, L.J., Arciniega, A., Greenwood, P.E., 2008. Construction of equivalent stochastic differential equation models. *Stochastic Anal. Appl.* 26, 274–297.
 Baxendale, P., Greenwood, P., 2011. Sustained oscillations for density dependent Markov processes. *J. Math. Biol.* 63, 433–457.
 Bliss, R., Painter, P., Marr, A., 1982. Role of feedback inhibition in stabilizing the classical operon. *J. Theor. Biol.* 97, 177–193.
 Chaffee, J., Kuske, R., 2011. The effect of loss of immunity on noise-induced sustained oscillations in epidemics. *Bull. Math. Biol.* 73, 2552–2574.
 Dallmann, R., Viola, A., Tarokh, L., Cajochoen, C., Brown, S., 2012. The human circadian metabolome. *Proc. Nat. Acad. Sci.* 109, 2625–2629.
 Dauxois, T., Di Patti, F., Fanelli, D., McKane, A., 2009. Enhanced stochastic oscillations in autocatalytic reactions. *Phys. Rev. E* 79, 036112.
 Davis, K., Roussel, M., 2006. Optimal observability of sustained stochastic competitive inhibition oscillations at organellar volumes. *FEBS J.* 273, 84–95.

- Dowse, H.B., 2008. Mid-range ultradian rhythms in *Drosophila* and the circadian clock problem. In: Lloyd, D., Rossi, E.L. (Eds.), *Ultradian Rhythms from Molecules to Mind*. Springer Netherlands, pp. 175–199.
- Elf, J., Ehrenberg, M., 2003. Fast evaluation of fluctuations in biochemical networks with the linear noise approximation. *Genome Res.* 13, 2475–2484.
- Gang, H., Ditzinger, T., Ning, C., Haken, H., 1993. Stochastic resonance without external periodic force. *Phys. Rev. Lett.* 71, 807–810.
- Gardiner, C., 2007. *Handbook of Stochastic Methods*. Springer.
- Geva-Zatorsky, N., Dekel, E., Batchelor, E., Lahav, G., Alon, U., 2010. Fourier analysis and systems identification of the p53 feedback loop. *Proc. Nat. Acad. Sci.* 107, 13550–13555.
- Gillespie, D., 1977. Exact stochastic simulation of coupled chemical reactions. *J. Phys. Chem.* 81, 2340–2361.
- Gillespie, D., 2000. The chemical Langevin equation. *J. Chem. Phys.* 113, 297.
- Gillespie, D., 2007. Stochastic simulation of chemical kinetics. *Annu. Rev. Phys. Chem.* 58, 35–55.
- Grima, R., 2009. Noise-induced breakdown of the Michaelis–Menten equation in steady-state conditions. *Phys. Rev. Lett.* 102, 218103.
- Grima, R., 2010. An effective rate equation approach to reaction kinetics in small volumes: theory and application to biochemical reactions in nonequilibrium steady-state conditions. *J. Chem. Phys.* 133, 035101.
- Grima, R., 2012. A study of the accuracy of moment-closure approximations for stochastic chemical kinetics. *J. Chem. Phys.* 136, 154105.
- Grima, R., Schnell, S., 2008. Modelling reaction kinetics inside cells. *Essays Biochem.* 45, 41.
- Grima, R., Thomas, P., Straube, A., 2011. How accurate are the nonlinear chemical Fokker–Planck and chemical Langevin equations? *J. Chem. Phys.* 135, 084103.
- Hou, Z., Xin, H., 2003. Internal noise stochastic resonance in a circadian clock system. *J. Chem. Phys.* 119, 11508.
- Klosek, M., Kuske, R., 2005. Multiscale analysis of stochastic delay differential equations. *Multiscale Model. Simulation* 3, 706–729.
- Ko, C., Yamada, Y., Welsh, D., Buhr, E., Liu, A., Zhang, E., Ralph, M., Kay, S., Forger, D., Takahashi, J., 2010. Emergence of noise-induced oscillations in the central circadian pacemaker. *PLoS Biol.* 8, e1000513.
- Kurtz, T., 1976. Limit theorems and diffusion approximations for density dependent Markov chains. In: *Stochastic Systems: Modeling, Identification and Optimization*, I. Springer, pp. 67–78.
- Kuske, R., Gordillo, L.F., Greenwood, P., 2007. Sustained oscillations via coherence resonance in SIR. *J. Theor. Biol.* 245, 459–469.
- Leise, T., Wang, C., Gitis, P., Welsh, D., 2012. Persistent cell-autonomous circadian oscillations in fibroblasts revealed by six-week single-cell imaging of PER2::LUC bioluminescence. *PLoS ONE* 7, e33334.
- Li, Q., Lang, X., 2008. Internal noise-sustained circadian rhythms in a *Drosophila* model. *Biophys. J.* 94, 1983–1994.
- Li, Q., Zhu, R., 2001. Stochastic resonance with explicit internal signal. *J. Chem. Phys.* 115, 6590.
- McKane, A., Nagy, J., Newman, T., Stefanini, M., 2007. Amplified biochemical oscillations in cellular systems. *J. Stat. Phys.* 128, 165–191.
- Mohawk, J., Green, C., Takahashi, J., 2012. Central and peripheral circadian clocks in mammals. *Annu. Rev. Neurosci.* 35, 445–462.
- Nagoshi, E., Saini, C., Bauer, C., Laroche, T., Naef, F., Schibler, U., 2004. Circadian gene expression in individual fibroblasts: cell-autonomous and self-sustained oscillators pass time to daughter cells. *Cell* 119, 693–705.
- Novák, B., Tyson, J., 2008. Design principles of biochemical oscillators. *Nat. Rev. Mol. Cell Biol.* 9, 981–991.
- Panda, S., Antoch, M., Miller, B., Su, A., Schook, A., Straume, M., Schultz, P., Kay, S., Takahashi, J., Hogenesch, J., 2002. Coordinated transcription of key pathways in the mouse by the circadian clock. *Cell* 109, 307–320.
- Qian, H., 2011. Nonlinear stochastic dynamics of mesoscopic homogeneous biochemical reaction systems—an analytical theory. *Nonlinearity* 24, R19.
- Ramaswamy, R., González-Segredo, N., Sbalzarini, I., Grima, R., 2012. Discreteness-induced concentration inversion in mesoscopic chemical systems. *Nat. Commun.* 3, 779.
- Reddy, A., Karp, N., Maywood, E., Sage, E., Deery, M., O'Neill, J., Wong, G., Chesham, J., Odell, M., Lilley, K., et al., 2006. Circadian orchestration of the hepatic proteome. *Curr. Biol.* 16, 1107–1115.
- Roenneberg, T., Chua, E.J., Bernardo, R., Mendoza, E., 2008. Modelling biological rhythms. *Curr. Biol.* 18 (17), R826–R835.
- Rozenfeld, A., Tessone, C., Albano, E., Wio, H., 2001. On the influence of noise on the critical and oscillatory behavior of a predator–prey model: coherent stochastic resonance at the proper frequency of the system. *Phys. Lett. A* 280, 45–52.
- Rozhnova, G., Nunes, A., 2009. Fluctuations and oscillations in a simple epidemic model. *Phys. Rev. E* 79, 041922.
- Schwanhäusser, B., Busse, D., Li, N., Dittmar, G., Schuchhardt, J., Wolf, J., Chen, W., Selbach, M., 2011. Global quantification of mammalian gene expression control. *Nature* 473, 337–342.
- Schwikowski, B., Uetz, P., Fields, S., 2000. A network of protein–protein interactions in yeast. *Nat. Biotechnol.* 18 (12), 1257–1261.
- Scott, M., 2012. Non-linear corrections to the time-covariance function derived from a multi-state chemical master equation. *IET Syst. Biol.* 6, 116.
- Simpson, M., Cox, C., Saylor, G., et al., 2004. Frequency domain chemical Langevin analysis of stochasticity in gene transcriptional regulation. *J. Theor. Biol.* 229, 383–394.
- Stratonovich, R., 1967. *Topics in the Theory of Random Noise*, vol. II. Gordon and Breach.
- Thomas, P., Straube, A., Grima, R., 2010. Stochastic theory of large-scale enzyme-reaction networks: finite copy number corrections to rate equation models. *J. Chem. Phys.* 133, 195101.
- Thomas, P., Matuschek, H., Grima, R., 2012. Computation of biochemical pathway fluctuations beyond the linear noise approximation using iNA. In: *2012 IEEE International Conference on Bioinformatics and Biomedicine (BIBM)*, IEEE, pp. 1–5. <http://dx.doi.org/10.1109/BIBM.2012.6392668>.
- Toner, D., Grima, R., 2013. Molecular noise induces concentration oscillations in chemical systems with stable node steady states. *J. Chem. Phys.* 138, 055101.
- Tyson, J., 2002. Biochemical oscillations. In: Fall, C.P., Marland, E.S., Wagner, J.M., Tyson, J.J. (Eds.), *Computational Cell Biology*. Springer, pp. 230–260.
- Tyson, J., Kauffman, S., 1975. Control of mitosis by a continuous biochemical oscillation: synchronization; spatially inhomogeneous oscillations. *J. Math. Biol.* 1, 289–310.
- Ushakov, O., Wünsche, H., Henneberger, F., Khovanov, I., Schimansky-Geier, L., Zaks, M., 2005. Coherence resonance near a Hopf bifurcation. *Phys. Rev. Lett.* 95, 123903.
- Van Kampen, N., 1976. The expansion of the master equation. *Adv. Chem. Phys.*, 245–309.
- van Kampen, N., 2007. *Stochastic Processes in Physics and Chemistry*, 3rd ed. North-Holland.
- Vilar, J., Kueh, H., Barkai, N., Leibler, S., 2002. Mechanisms of noise-resistance in genetic oscillators. *Proc. Nat. Acad. Sci.* 99, 5988–5992.
- Wallace, E., Gillespie, D., Sanft, K., Petzold, L., 2012. Linear noise approximation is valid over limited times for any chemical system that is sufficiently large. *IET Syst. Biol.* 6, 102–115.
- Warren, P., Tanase-Nicola, S., ten Wolde, P., et al., 2006. Exact results for noise power spectra in linear biochemical reaction networks. *J. Chem. Phys.* 125, 144904.
- Welsh, D., Yoo, S., Liu, A., Takahashi, J., Kay, S., 2004. Bioluminescence imaging of individual fibroblasts reveals persistent, independently phased circadian rhythms of clock gene expression. *Curr. Biol.* 14, 2289–2295.
- Westermark, P., Welsh, D., Okamura, H., Herzog, H., 2009. Quantification of circadian rhythms in single cells. *PLoS Comput. Biol.* 5, e1000580.
- Zhong, S., Qi, F., Xin, H., 2001. Internal stochastic resonance in a model system for intracellular calcium oscillations. *Chem. Phys. Lett.* 342, 583–586.
- Zinn-Justin, J., 2007. *Phase Transitions and Renormalization Group*. Oxford University Press.